AD_____

Award Number: W81XWH-10-1-0742

TITLE: A Brain-Machine-Brain Interface for Rewiring of Cortical Circuitry after Traumatic Brain Injury

PRINCIPAL INVESTIGATOR: Randolph J. Nudo, PhD

CONTRACTING ORGANIZATION: University of Kansas Medical Center Research Kansas City, KS 66103-2937

REPORT DATE: September 2014

TYPE OF REPORT: Annual

PREPARED FOR: U.S. Army Medical Research and Materiel Command
Fort Detrick, Maryland 21702-5012

DISTRIBUTION STATEMENT:

× Approved for public release; distribution unlimited

REPORT DOCUMENTATION PAGE

Form Approved
OMB No. 0704-0188

1. REPORT DATE *(DD-MM-YYYY)*	2. REPORT TYPE	3. DATES COVERED *(From - To)*
September 2014	Annual	01 Sep 2013 – 31 Aug 2014

4. TITLE AND SUBTITLE
A Brain-Machine-Brain Interface for Rewiring of Cortical Circuitry after Traumatic Brain Injury

5a. CONTRACT NUMBER

5b. GRANT NUMBER
W81XWH-10-1-0742

5c. PROGRAM ELEMENT NUMBER

6. AUTHOR(S)

Randolph J. Nudo, PhD

email:rnudo@kumc.edu

5d. PROJECT NUMBER

5e. TASK NUMBER

5f. WORK UNIT NUMBER

7. PERFORMING ORGANIZATION NAME(S) AND ADDRESS(ES)

University of Kansas Medical Center Research
3901 Rainbow Boulevard, MSN 1039
Kansas City, KS 66103-2937

8. PERFORMING ORGANIZATION REPORT NUMBER

9. SPONSORING / MONITORING AGENCY NAME(S) AND ADDRESS(ES)
U.S. Army Medical Research and Materiel
Command Fort Detrick Maryland 21702-5012

10. SPONSOR/MONITOR'S ACRONYM(S)

11. SPONSOR/MONITOR'S REPORT NUMBER(S)

12. DISTRIBUTION / AVAILABILITY STATEMENT

Approved for public release; distribution unlimited

13. SUPPLEMENTARY NOTES

14. ABSTRACT

A small, lightweight microdevice has been developed for activity-dependent stimulation (ADS) and successfully tested for functionality in both anesthetized and ambulatory rats. Further, in semi-chronic experiments in rats with TBI using this microsystem, an unprecedented, potent effect of ADS on motor performance has been demonstrated, as compared to control rats (injured but no microdevice) and open-loop stimulation (OLS) rats. Specifically, open-loop stimulation does result in some recovery after injury, but ADS is significantly more efficacious, resulting in recovery to normal ranges of performance within 2 weeks after injury. In the final stage of this funding period, we will prepare to extend these findings to non-human primates as we finalize a) the optimal parameters for the primate TBI model and b) the design and construction of the primate microdevice.

15. SUBJECT TERMS
Anatomical rewiring; Implantable microsystem; Neuroplasticity; Rehabilitation; Traumatic brain injury

16. SECURITY CLASSIFICATION OF:			17. LIMITATION OF ABSTRACT	18. NUMBER OF PAGES	19a. NAME OF RESPONSIBLE PERSON
a. REPORT	b. ABSTRACT	c. THIS PAGE			USAMRMC
U	U	U	UU	36	19b. TELEPHONE NUMBER *(include area code)*

Table of Contents

Page

A Brain-Machine-Brain Interface for Rewiring of Cortical Circuitry after Traumatic Brain Injury

Award Number W81XWH-10-1-0742
Randolph J. Nudo, PhD
Annual Report
February 2015

Introduction

The goal of this project is to use an implantable brain-machine-brain interface to enhance behavioral recovery after traumatic brain injury by reshaping long-range intracortical connectivity patterns. We hypothesize that artificial synchronous activation of distant cortical locations will encourage spontaneously sprouting axons to migrate toward and terminate in the coupled region, and that such directed sprouting can aid in functional recovery.

Body

Substantial progress has been made in demonstrating proof-of-concept for our approach in a rodent model of traumatic brain injury. The Tasks at Kansas University Medical Center comprise the neurobiology components of the collaborative project with investigators at Case Western Reserve University who are performing the electronics and microsystem packaging components. In the first quarter of Year 4, we published our primary findings showing rapid recovery of motor abilities in rats implanted with the microdevice in the journal *The Proceedings of the National Academy of Science* (PNAS). During the ensuing weeks, the study attracted considerable attention from various news agencies, technology leaders in the microelectronics field, and was featured on the CDMRP's own website.

The algorithms developed during the course of the manuscript revision have proved to be very enlightening. During Year 3, we revisited our Year 1 parameter optimization experiments that were proposed in acute, anesthetized rat preparations. These studies (requiring no new animals or modification of approved procedures) yielded new information on the rapidity and specificity of activity-dependent stimulation that will help guide the further development of this novel approach.

Finally, we worked with the engineering group at Case Western Reserve University to progress in the design of the primate microdevice. We also initiated pilot studies in non-human primates required by our local IACUC before proceeding with the full primate series. These pilot studies were funded by internal KUMC sources, and thus, not subject to approval by ACURO. The full primate series has received full ACURO approval, and the non-human primate model development can now proceed.

In the text that follows, we describe the research accomplishments associated with tasks from previous phases as outlined in the approved Statement of Work.

Phase I (1-12 months), Task 2 (Neurobiology)

2.3 Analyze evoked spike discharges to determine optimal time delays (i.e., delays corresponding to maximum potentiation).

While the initial goal of these experiments was the optimization of spike-stimulus delays, the rapid potentiation found with activity-dependent stimulation, but not open-loop stimulation, demonstrated that we can examine many parameters in anesthetized preparations relatively quickly. All local and ACURO approval was received for these studies. The results of this analysis demonstrated that functional connectivity could be enhanced within hours in an anesthetized rat after controlled cortical impact. Several other ancillary results have shed insight into the specificity of these effects, both at the level of the cortical area of interest, as well as the specific set of neurons used to trigger the stimulation.

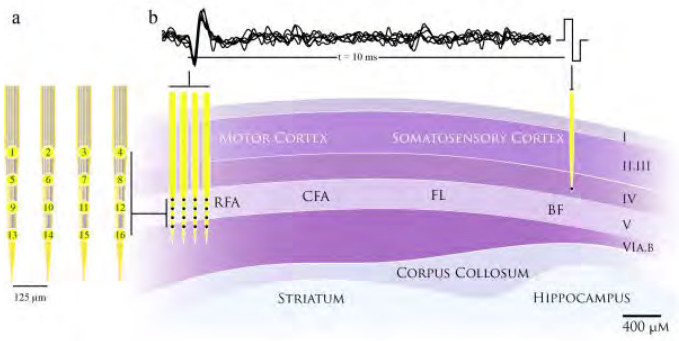

Two stimulation paradigms - activity-dependent stimulation (ADS) and random stimulation (RS) - were applied to the rat cortex. ADS utilized action potentials recorded from one of 16 electrode contacts in RFA (Figure 1a) to trigger single 60 µA stimulus pulses to either the S1 forelimb area (FL) or barrel field (BF) (Figure 1b). RS delivered single 60 µA stimulus pulses at random intervals at a mean frequency of 7 Hz (firing frequency of ADS stimulus pulses) to either FL or BF. The resultant stimulus-associated action potentials (spikes) recorded at short latency within RFA were used as an indication of a functional connection between FL and RFA or between BF and RFA. Each stimulation paradigm was applied in 8 individual animals, for a total of 16 animals, and each data session lasted for three one-hour stimulation periods interspersed by ten-minute periods with no stimulation.

Figure 2 shows the mean number of spikes per stimulus pulse recorded during the 28 ms directly following each stimulus pulse, for ADS (Figure 2A) and RS (Figure 2b) conditions pooled from all animals in the study. Stimulus-associated spikes, calculated as the mean number of spikes per stimulus, were used to allow inter-session comparison by normalizing for the total number of stimulus pulses delivered across sessions. All spikes recorded at the 16 electrode contacts were used to calculate the mean spikes per stimulus (y-axis), subdivided into 1 ms bins for the 28 ms following each stimulus pulse (x-axis). Baseline neural activity prior to simulation is indicated by the horizontal dashed line. In the ADS condition, the data indicate a distinct peak above baseline firing rates within the first 10 ms following stimulus onset, and a return to baseline firing rates by the end of the 28 ms. In contrast, there was minimal increase above baseline in the RS condition. The mean number of spikes per stimulus in the 28ms post-stimulus period, pooled across all data in ADS and RS conditions, respectively, was significantly greater for the ADS condition (0.11 ± 0.13 spikes/stimulus) than in the RS condition (0.06 ± 0.09 spikes/stimulus, Mann-Whitney U Statistic 1541.5; p = 0.016). Greater cumulative spikes for ADS, compared to RS conditions, combined with the short-latency peak in spike rate, suggests a stronger facilitatory response to stimulation and a more potent cortico-cortical potentiation than for RS.

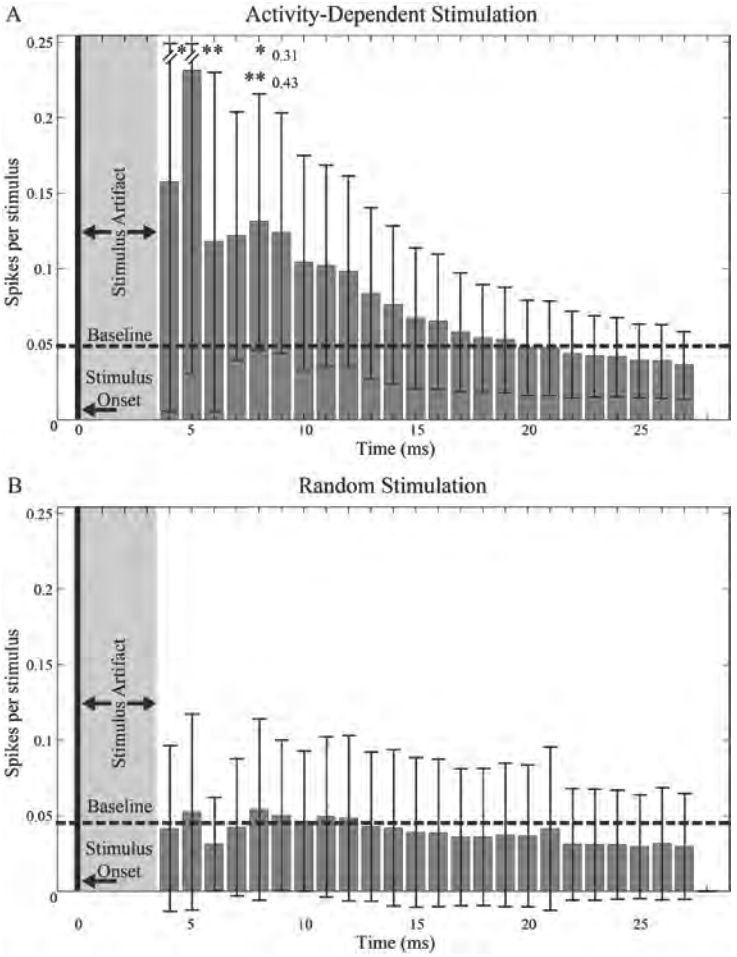

Figure 2 Cumulative ADS- versus RS-associated neural activity for all recording sessions.

There were also different effects of ADS depending upon what cortical area was stimulated (Figure 3). These data reveal that subjects in the BF-RFA group displayed more stimulus-associated spikes relative to baseline (set to 0), compared to those in FL-RFA which had a moderate *decrease* in spikes relative to baseline. These data suggest that ADS promotes excitatory connectivity between RFA and BF, but an inhibitory one between RFA and FL.

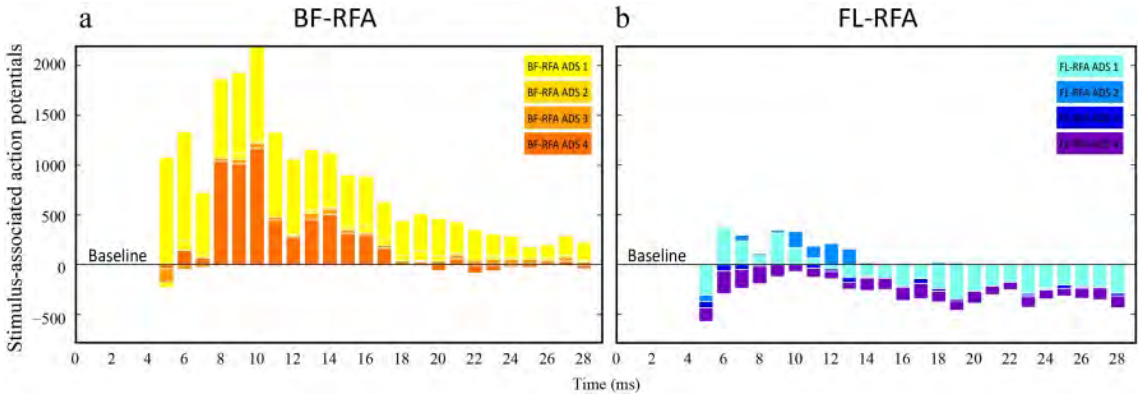

Figure 3 ADS-associated RFA neural activity in BF (a) and FL (b). Each color represents data collected from a single animal spanning the recording session.

Thus, ADS enhances long-term potentiation or depression depending upon the connection source. We found that ADS facilitated inhibitory FL-RFA connectivity and excitatory BF-RFA connectivity. This distinction may be associated with more robust pre-existing connectivity between FL-RFA, in comparison to BF-RFA. It is possible that in the case of FL-RFA, inhibitory GABAergic connectivity was promoted, thereby decreasing the target RFA activity over time. In contrast, BF-RFA has less pre-existing direct connectivity. This may encourage the encoding of new cortico-cortical circuits from BF to RFA, thereby requiring creation of a novel pathway. It is possible, therefore, that ADS promoted connectivity from BF to RFA by enhancing LTP through previously indirect synaptic connections.

Finally, the effects of ADS appear to be highly spatially specific based on the channel used to trigger the stimulation. Pooling all data collected in ADS-BF sessions, the mean stimulus-associated action potentials recorded in the trigger channels in RFA (0.27 ± 0.19 spikes/stimulus) was significantly greater than the action potentials recorded on the remaining RFA channels (0.10 ± 0.12 spikes/stimulus, Mann-Whitney U Statistic = 39.0; p = 0.026; Figure 4). Similarly, pooling data collected in ADS-FL sessions, the mean stimulus-associated action potentials recorded in the trigger channels in RFA (0.19 ± 0.18 spikes/stimulus) was significantly greater than the action potentials recorded on the remaining RFA channels (0.06 ± 0.09 spikes/stimulus). These data were presented in an oral abstract at the 2014 Society for Neuroscience meeting (appendix). A manuscript is near completion.

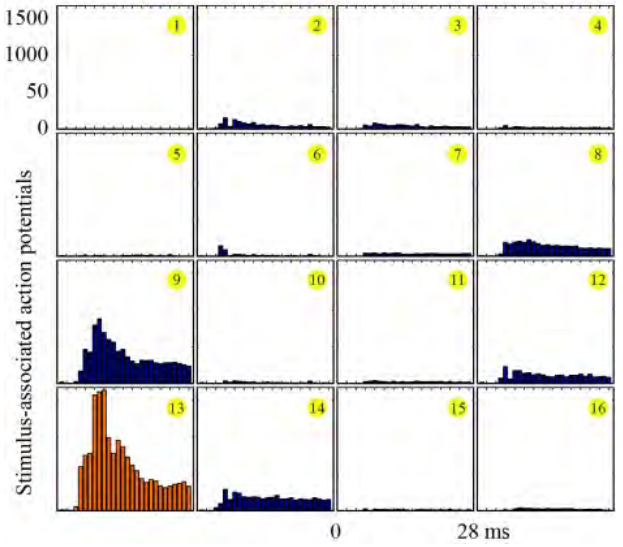

Figure 4 *ADS-associated spikes in each of the 16 channels*

<u>Phase II (13-24 months), Task 3 (Neurobiology)</u>

3.1 through 3.11 Test microdevice in rats with TBI

As mentioned in a previous report, rapid recovery was found in rats receiving activity-dependent stimulation. The major accomplishment on this task in Year 4 was the publication of the report in *PNAS*. Our approach was to functionally link the neural activity of the premotor (PM) forelimb area (RFA) with activation of the S1 forelimb area following a controlled cortical impact (CCI) to M1 (Figure 5B, C). To this end, a microdevice was developed with the ability to deliver activity-dependent stimulation (ADS) through recording and digitizing extracellular neural activity from an implanted microelectrode, discriminating individual action potentials (spikes), and delivering small amounts of electrical current to another microelectrode implanted in a distant population of neurons. This closed-loop system was similar, in principle, to the "Neurochip", used

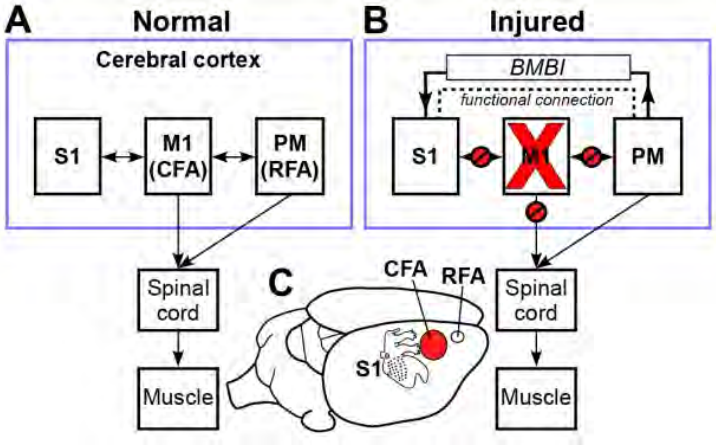

Figure 5 Experimental paradigm for restoration of function using a BMBI.

previously by other investigators to demonstrate the effects of local ADS in intact animals, but was miniaturized for head-mounted, wireless operation. By linking the activity of one area of the cortex with that of a distant one, a closed-loop brain-machine-brain interface (BMBI) for artificial corticocortical communication between PM and S1 was created.

Individual spikes were detected in PM and subsequent stimulation was delivered to S1 after a 7.5 ms delay. After the M1 injury, rats were implanted with microelectrodes connected to the BMBI microdevice. The microdevice delivered ADS 24 hours per day up to 28 days post-injury, except for brief motor assessment sessions on predetermined days. Behavioral recovery in ADS rats was compared to recovery in rats with open-loop stimulation (OLS), in which S1 stimulation was uncorrelated with spikes in PM, and to control rats that had no microdevice implanted.

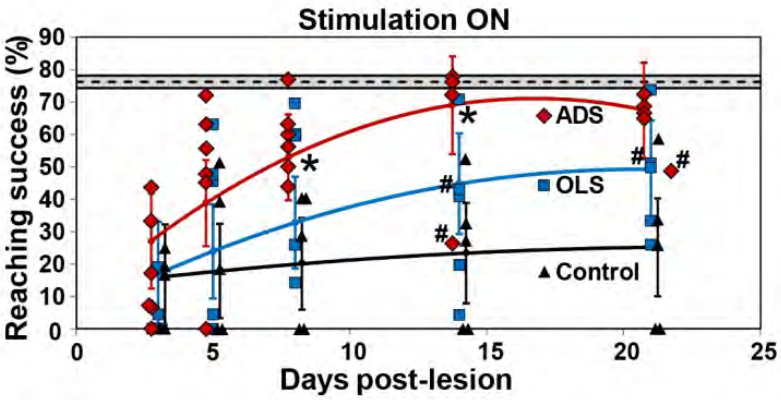

Figure 6 Behavioral results of ADS treatment.

Rats in each of the three groups demonstrated a severe deficit on the skilled reaching task in the first few days after the injury (Figure 6). On post-lesion Days 3 and 5, there were no significant differences in motor performance among the groups (Global comparisons: $p = 0.5265$ and 0.0945, respectively). Rats in the Control group (with lesion, but no microdevice) continued to demonstrate a profound deficit that plateaued at only about 25% successful retrievals. In striking contrast, by post-lesion Day 8, group performance was significantly different (Global comparison: $p = 0.0044$). Rats in the ADS group showed a substantial and statistically significant behavioral improvement in reaching success compared to the other groups in the ON condition (Pairwise comparisons: $p = 0.0418$ for ADS vs. OLS; $p = 0.0012$ for ADS vs. Control; and $p = 0.2110$ for OLS vs. Control; Figure 6). By post-lesion Day 14, the performance of the rats in the ADS group was approximately at pre-lesion levels, and significantly higher than the other groups. The difference between the OLS group and the Control group approached significance on Day 14. (Global comparison: $p = 0.0004$; Pairwise comparisons: $p = 0.0284$ for ADS vs. OLS; $p < 0.0001$ for ADS vs. Control; $p = 0.0555$ for OLS vs. Control). By post-lesion Day 21, performance in the ADS group remained high and statistically different from that of the Control group. Performance was not significantly different in the ADS group between Day 14 and 21 ($p = 0.576$). However, by Day 21, the OLS group had improved further so that the difference between the two groups was not significant (Global comparison: $p = 0.0007$; Pairwise comparisons: $p = 0.0891$ for ADS vs. OLS; $p = 0.0002$ for ADS vs. Control; $p = 0.0278$ for OLS vs. Control).

To explore possible neurophysiological mechanisms underlying the behavioral effects of the ADS treatment on post-injury motor performance, we performed post-hoc analysis of spike events in RFA that were discriminated in the 28 ms after each S1 stimulus pulse. Post-stimulus spike histograms were compared to 28 ms periods chosen from data acquired in the OFF condition after each S1 stimulus pulse. The results show that substantially more spikes in RFA occurred following S1 stimulation in the ADS group, with peak activity occurring approximately 4-6 ms after the S1 stimulus pulse (Figure 7). Spike rates were nearly 3 times higher averaged across the 28 ms period, compared with a comparable period in the OFF condition. Spike rates in the OLS group were slightly lower than the ADS group in the OFF condition, but were significantly lower than the ADS group in the ON condition. These data suggest that ADS substantially reinforced network interactions between S1 and RFA, while OLS did not. Subdividing the spike histograms by Day reveals that enhanced spike activity in the ADS ON condition is evident even on the first day that the microdevice was activated (Figure 7B). Also, there is a trend toward further increases in spike discharge between the first (Days 5 and 8) and second (Days 8 and 14) week in the ADS group, corresponding to the time period when behavioral performance approached normal levels.

This proof-of-concept study now published in *PNAS* (Guggenmos et al., 2013) demonstrates that neural interface systems can be used effectively to functionally bridge damaged neural pathways and promote recovery after brain injury.

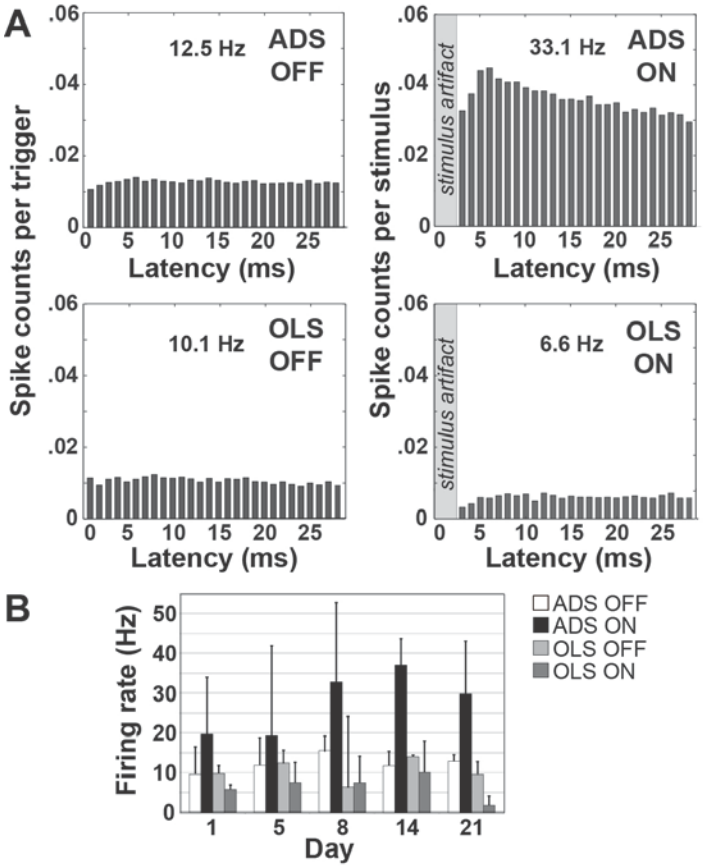

Figure 7 Synaptic facilitation after ADS treatment.

Phase III (25-36 months), Task 3 (Neurobiology)

3.1 through 3.6 Determine anatomical changes in connectivity

Our original plan was to examine anatomical connectivity that could be altered by activity-dependent stimulation in our Phase II study. However, the placement of the microelectrodes in the cerebral cortex interfered with the tract-tracing protocol, and, while we could demonstrate some connectivity, the anatomical data was not viable for quantitative analysis for comparison among groups. Also, as a result of an NIH-funded project in our laboratory investigating anatomical connectivity in a rat stroke model, we found that the normal rat connectivity patterns with the premotor area, the focus of our anatomical studies, are more diffuse than we found for non-human primates. Thus, the previously proposed anatomical experiment is underpowered for the quantitative analysis required. As noted in the Year 3 progress report, a separate experiment to identify anatomical changes, if they exist, was proposed. The revised protocol requesting additional rats for this purpose was approved by our local IACUC and subsequently, by ACURO during Year 4.

In addition, we recruited a post-doctoral fellow to conduct these experiments, and to train for our non-human primate studies. Heather Hudson, Ph.D. arrived in August 2014, and has extensive experience using single-neuron recording techniques in primates, and has now developed the surgical and technical skills to conduct the anatomical studies in rats. Due to her arrival date, we plan to complete the anatomical experiments during the no-cost extension year (i.e., Year 5).

Phase IV (37-48 months), Task 2 (Neurobiology)

We completed all review and approval processes for non-human primate studies. Approval has been obtained both from our local IACUC committee as well as ACURO. This included the 3-year *de novo* review

process. An on-site inspection of the KUMC facility by DoD veterinarians was conducted, and the site was approved for the studies. We are proceeding with the development of the non-human primate TBI model, as approved. First, we need to establish parameters for the impact injury. Then, we will perform that full study.

We plan to conduct the full primate study as originally designed, but after we have optimized impact parameters. As noted previously, very few non-human primate studies have ever been done using the controlled cortical impact model that is common in rodents. Thus, it is important to proceed with such studies carefully. We fully intend to complete the entire study as proposed, even though it is likely to extend beyond the period of the current funding.

During Year 4, we also continued to work with the engineering team at Case Western Reserve University to finalize the non-human primate devices. Construction of the plastic chambers that will be used to house the microdevice was completed in Q1 and delivered to the neurobiology team. This was a collaborative effort between the neurobiological team at KUMC and the engineering team at Case Western Reserve University.

Key Research Accomplishments

- Published paper describing main proof-of-principle results in rats with TBI.
- Completed all regulatory requirements to for revised non-human primate protocol.
- Presented functional connectivity data in anesthetized rats with TBI orally at Society for Neuroscience meeting.
- Prepared manuscript describing functional connectivity data in anesthetized rats with TBI.
- Completed regulatory review for 3-year *de novo* review at local IACUC, and received approval from ACURO

Reportable Outcomes

1- Manuscripts/Abstracts/Presentations:

- Guggenmos DJ, M Azin, S Barbay, JD Mahnken, C Dunham, P Mohseni, and RJ Nudo, "Restoration of function after brain damage using a neural prosthesis," Proc. Natl. Acad. Sci. USA (PNAS), vol. 110, no. 52, pp. 21177-21182, December 2013.
- Van Acker GM, Guggenmos D, Pack A, Dunham C, Nudo RJ (2013) Potentiating functional connectivity between distant cortical locations with activity dependent stimulation in the anesthetized rat. Program No. 79.06. 2013 Neuroscience Meeting Planner. New Orleans, LA. Society for Neuroscience, 2013. Online.
- Guggenmos DJ, C Dunham, M Azin, S Barbay, JD Mahnken, P Mohseni and RJ Nudo (2013) Neurophysiological effects of activity-dependent stimulation following a controlled cortical impact to primary motor cortex of the rat. Program No. 79.12. 2013 Neuroscience Meeting Planner. New Orleans, LA. Society for Neuroscience, 2013. Online.
- Van Acker, GM, Guggenmos D, Barbay S, Crabtree K, Dunham C, Nudo RJ (2014) Inducing cortico-cortical connectivity to bypass acute cortical impact injury in the rat. Program N. 17.08. 2014 Neuroscience Meeting Planner. Washington, DC. Society for Neuroscience, 2014, Online (submitted during Year 4).
- Nudo, RJ, "Shaping plasticity to enhance recovery after injury", World Congress of Neurology, Vienna, Austria, September 22, 2013
- Nudo, RJ, "Plasticity of Brain Networks and Relationship to Recovery after Injury", Brain Research Centre, University of British Columbia, Vancouver, Canada, October 11, 2013.
- Nudo, RJ, "Development and application of a closed-loop neural prosthesis to potentiate functional connectivity and restore function after cortical injury". 2014 Australasian Neuroscience Society, Adelaide, Australia, January 31, 2014.

- Nudo, RJ, “Neuroprosthetic tools for repair of the injured brain”, Winter Conference on Neural Plasticity, Vieques, Puerto Rico, February 27, 2014.
- Nudo, RJ, “Neuroprosthetic tools for repair of the injured brain”, 4th Scientific Conference "Restauración Neurológica 2014, Havana, Cuba, March 6, 2014.
- Nudo, RJ, Keynote Address, “Neuroprosthetic tools for repair of the injured brain”, Conference on Systems Neuroscience and Rehabilitation, Tokyo, Japan, March 13, 2014.
- Nudo, RJ, “Neuroprosthetic tools for repair of the injured brain” Burke-Cornell Medical Research Institute Weekly Colloquium, White Plains, New York, March 25, 2014.
- Nudo, RJ, “Neuroprosthetic tools for repair of the injured brain” Rehabilitation Institute of Chicago, Chicago, Illinois, April 4, 2014.
- Nudo RJ, “Neuroprosthetic tools for repair of the injured brain” University of Missouri School of Health Professions Scholarship and Discovery Lecture Series, April 11, 2014.
- Nudo, RJ “Neuroprosthetic tools for repair of the injured brain” 36th Symposium of the GRSNC: Sensorimotor Rehabilitation: At the crossroad of the Basic and Clinical Sciences, University of Montreal, Montreal Canada, May 13, 2014.
- Nudo, RJ, “Neuroprosthetic tools for repair of the injured brain” III Workshop of Synaptic Plasticity: From Bench to Bedside, Milazzo, Sicily, June 2014.

2- Patents and Licenses Applied for/Issued: None issued.

3- Degrees Obtained from Award: None.

4- Development of Cell Lines and Tissue/Serum Repositories: Not applicable.

5- Informatics (Databases and Animal Models): None yet.

6- Funding Applied for: W81XWH-14-SCIRP-IIRA (Spinal Cord Injury Research Program – Investigator-Initiated Research Award) – Currently pending

7- Employment/Research Opportunities Applied for/Received: None yet.

Conclusion

Rapid progress is being made toward developing smart prosthetic platforms for altering plasticity in the injured brain, leading to future therapeutic interventions for TBI that are guided by the underlying mechanisms for long-range functional and structural plasticity in the cerebral cortex. An unprecedented, potent effect of activity-dependent stimulation (ADS) on motor performance has been demonstrated in rats with TBI. Neurophysiological evidence suggests that functional connectivity between the target areas is enhanced by activity-dependent stimulation. Design of the device, and pilot experiments for non-human primates are underway.

Appendix I Guggenmos DJ, M. Azin, S. Barbay, J. D. Mahnken, C. Dunham, P. Mohseni, and R. J. Nudo, “Restoration of function after brain damage using a neural prosthesis,” Proc. Natl. Acad. Sci. USA (PNAS), vol. 110, no. 52, pp. 21177-21182, December 2013.

Appendix II Van Acker GM, Guggenmos D, Pack A, Dunham C, **Nudo RJ** (2013) Potentiating functional connectivity between distant cortical locations with activity dependent stimulation in the anesthetized rat. Program No. 79.06. 2013 Neuroscience Meeting Planner. New Orleans, LA. Society for Neuroscience, 2013. Online.

Appendix III Guggenmos DJ, C Dunham, M Azin, S Barbay, JD Mahnken, P Mohseni and RJ Nudo (2013) Neurophysiological effects of activity-dependent stimulation following a controlled cortical impact to primary motor cortex of the rat. Program No. 79.12. 2013 Neuroscience Meeting Planner. New Orleans, LA. Society for Neuroscience, 2013. Online.

Appendix IV Van Acker, GM, Guggenmos D, Barbay S, Crabtree K, Dunham C, Nudo RJ (2014) Inducing cortico-cortical connectivity to bypass acute cortical impact injury in the rat. Program N. 17.08. 2014 Neuroscience Meeting Planner. Washington, DC. Society for Neuroscience, 2014, Online (submitted during Year 4).

Restoration of function after brain damage using a neural prosthesis

David J. Guggenmos[a,b,1], Meysam Azin[c,2], Scott Barbay[a,b], Jonathan D. Mahnken[d], Caleb Dunham[a,b], Pedram Mohseni[c], and Randolph J. Nudo[a,b,3]

Departments of [a]Molecular and Integrative Physiology and [d]Biostatistics, and [b]Landon Center on Aging, Kansas University Medical Center, Kansas City, KS 66160; and [c]Department of Electrical Engineering and Computer Science, Case Western Reserve University, Cleveland, OH 44106

Edited* by Michael Merzenich, Brain Plasticity Institute, San Francisco, CA, and approved November 15, 2013 (received for review September 6, 2013)

Neural interface systems are becoming increasingly more feasible for brain repair strategies. This paper tests the hypothesis that recovery after brain injury can be facilitated by a neural prosthesis serving as a communication link between distant locations in the cerebral cortex. The primary motor area in the cerebral cortex was injured in a rat model of focal brain injury, disrupting communication between motor and somatosensory areas and resulting in impaired reaching and grasping abilities. After implantation of microelectrodes in cerebral cortex, a neural prosthesis discriminated action potentials (spikes) in premotor cortex that triggered electrical stimulation in somatosensory cortex continuously over subsequent weeks. Within 1 wk, while receiving spike-triggered stimulation, rats showed substantially improved reaching and grasping functions that were indistinguishable from prelesion levels by 2 wk. Post hoc analysis of the spikes evoked by the stimulation provides compelling evidence that the neural prosthesis enhanced functional connectivity between the two target areas. This proof-of-concept study demonstrates that neural interface systems can be used effectively to bridge damaged neural pathways functionally and promote recovery after brain injury.

brain–machine–brain interface | neural plasticity | traumatic brain injury | closed-loop | long-term potentiation

The view of the brain as a collection of independent anatomical modules, each with discrete functions, is currently undergoing radical change. New evidence from neurophysiological and neuroanatomical experiments in animals, as well as neuroimaging studies in humans, now suggests that normal brain function can be best appreciated in the context of the complex arrangements of functional and structural interconnections among brain areas. Although mechanistic details are still under refinement, synchronous discharge of neurons in widespread areas of the cerebral cortex appears to be an emergent property of neuronal networks that functionally couple remote locations (1). It is now recognized that not only are discrete regions of the brain damaged in injury or disease but, perhaps more importantly, the interconnections among uninjured areas are disrupted, potentially leading to many of the functional impairments that persist after brain injury (2). Likewise, plasticity of brain interconnections may partially underlie recovery of function after injury (3).

Technological efforts to restore brain function after injury have focused primarily on modulating the excitability of focal regions in uninjured parts of the brain (4). Purportedly, increasing the excitability of neurons involved in adaptive plasticity expands the neural substrate potentially involved in functional recovery. However, no methods are yet available to alter the functional connectivity between spared brain regions directly, with the intent to restore normal communication patterns. The present paper tests the hypothesis that an artificial communication link between uninjured regions of the cerebral cortex can restore function in a rodent model of traumatic brain injury (TBI). Development of such neuroprosthetic approaches to brain repair may have important implications for the millions of individuals who are left with permanent motor and cognitive impairments after acquired brain injury, as occurs in stroke and trauma.

For the present experiment, we used a rodent model of focal brain injury to the caudal forelimb area (CFA), a region that is part of the cortical sensorimotor system. This area in the frontal cortex shares many properties with primary motor cortex (M1) of primates; injury to M1 results in long-term impairment in reaching and grasping functions (5). Traditionally, it has been thought that impairment occurs because M1 provides substantial outputs to the motor apparatus in the spinal cord, thus directly affecting motor output function. However, M1 also has important interconnections with the primary somatosensory cortex (S1) located in the parietal lobe (Fig. 1*A*). Long-range corticocortical fibers from S1 provide critical information to M1 about the position of the limb in space. Thus, injury to M1 results in impaired motor performance due, at least in part, to disruption in communication between the somatosensory and motor cortex (6).

To test our hypothesis that functional recovery can be facilitated by creating an artificial communication link between spared somatosensory and motor regions of the brain, we focused on the rat's premotor cortex (PM). The rostral forelimb area (RFA) is a premotor area in the rodent's frontal cortex that shares many properties with PM of primates and is thought to participate in recovery of function after injury to M1 (5, 7–9). PM areas are so-named because the principal target of their output fibers is M1 (10). PM areas also have long-range corticocortical connections with somatosensory areas, but at least in

Significance

Closed-loop systems, or brain–machine–brain interfaces (BMBIs), have not been widely developed for brain repair. In this study, we targeted spared motor and somatosensory regions of the rat brain after traumatic brain injury for establishment of a functional bridge using a battery-powered microdevice. The results show that by using discriminated action potentials as a trigger for stimulating a distant cortical location, rapid recovery of fine motor skills is facilitated. This study provides strong evidence that BMBIs can be used to bridge damaged neural pathways functionally and promote recovery after brain injury. Although this study is restricted to a rodent model of TBI, it is likely that the approach will also be applicable to other types of acquired brain injuries.

Author contributions: D.J.G., M.A., P.M., and R.J.N. designed research; D.J.G., M.A., and S.B. performed research; D.J.G., M.A., J.D.M., C.D., P.M., and R.J.N. analyzed data; and D.J.G., M.A., J.D.M., P.M., and R.J.N. wrote the paper.

The authors declare no conflict of interest.

*This Direct Submission article had a prearranged editor.

Freely available online through the PNAS open access option.

[1]Present address: Department of Neurobiology, Duke University, Durham, NC 27705.

[2]Present address: Qualcomm CDMA Technologies, Qualcomm, Inc., San Diego, CA 92121.

[3]To whom correspondence should be addressed. E-mail: rnudo@kumc.edu.

This article contains supporting information online at www.pnas.org/lookup/suppl/doi:10.1073/pnas.1316885110/-/DCSupplemental.

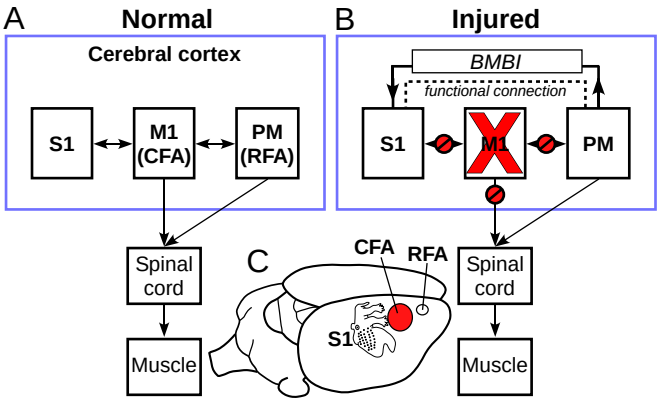

Fig. 1. Theoretical model of neuroprosthetic treatment approach after brain injury. (*A*) Normal connectivity of M1, S1, and PM. Both M1 (CFA in rat) and PM (RFA in rat) send substantial outputs to the spinal cord via the corticospinal tract. Also, extensive reciprocal connections exist between M1 and PM, as well as between M1 and S1. (*B*) Effects of focal M1 injury on brain connectivity and the hypothetical effect of a BMBI to restore somatosensory-motor communication. An injury to M1, as might occur in stroke or brain trauma, results in a focal area of necrosis, as well as loss of M1 outputs to the spinal cord. Corticocortical communication between M1 and S1 (and between M1 and PM) is also disrupted, further contributing to functional impairment. Because the uninjured PM also contains corticospinal neurons, it might have the ability to serve in a vicarious role. The dotted line indicates enhanced functional connection between PM and S1 that we propose is established after treatment with a BMBI. (*C*) Location of target areas in rat cerebral cortex. A topographic map of the somatosensory representation in S1 is superimposed on the cortex.

intact animals, they appear to be relatively weak compared with M1's connections with the somatosensory cortex (9, 11, 12).

Our approach was to link the neural activity of the PM forelimb area (RFA) functionally with activation of the S1 forelimb area following a controlled cortical impact (CCI) to M1 (Fig. 1 *B* and *C*). To this end, a microdevice was developed with the ability to deliver activity-dependent stimulation (ADS) through recording and digitizing extracellular neural activity from an implanted microelectrode, discriminating individual action potentials (spikes), and delivering small amounts of electrical current to another microelectrode implanted in a distant population of neurons (13, 14). This closed-loop system was similar, in principle, to the "Neurochip" used previously by other investigators to demonstrate the effects of local ADS in intact animals (15), but it was miniaturized for head-mounted, wireless operation (Fig. 2*A* and Fig. S1). By linking the activity of one area of the cortex with that of a distant area of the cortex, a closed-loop brain–machine–brain interface (BMBI) for artificial corticocortical communication between PM and S1 was created.

Individual spikes were detected in PM, and subsequent stimulation was delivered to S1 after a 7.5-ms delay (Fig. 2*B*). (Because connections between distant cortical areas are commonly reciprocal, enhanced communication theoretically could be established by ADS in either direction.) After the M1 injury, rats were implanted with microelectrodes connected to the BMBI microdevice (Fig. 2*A*). The microdevice delivered ADS 24 h per day up to 28 d postinjury, except for brief motor assessment sessions on predetermined days. Behavioral recovery in ADS rats was compared with recovery in rats with open-loop stimulation (OLS), in which S1 stimulation was uncorrelated with spikes in PM, and with control rats that had no microdevice implanted.

Results

Testing Motor Skill After Brain Injury. The primary behavioral assay for determining whether ADS resulted in functional improvement after brain injury was a skilled reaching task. This widely used task is a particularly sensitive measure of forelimb motor function after M1 lesions in both rodents and primates. Rats were pretrained to achieve a minimum criterion score of >70% successful pellet retrievals. After the lesion was created, rats were tested on the task during assessment sessions on postlesion days 3, 5, 8, 14, 21, and 28. During each postlesion assessment session, rats were tested under two conditions: first with the microdevice stimulation function turned OFF and then with the stimulation function turned ON. Rats in each of the three groups demonstrated a severe deficit on the skilled reaching task in the first few days after the injury (Fig. 3). On postlesion days 3 and 5, there were no significant differences in motor performance between the groups (global comparisons: $P = 0.5265$ and $P = 0.0945$, respectively). Rats in the control group (with a lesion but no microdevice) continued to demonstrate a profound deficit that plateaued at only about 25% successful retrievals. In striking contrast, by postlesion day 8, group performance was significantly different (global comparison: $P = 0.0044$). Rats in the ADS group showed a substantial and statistically significant behavioral improvement in reaching success compared with rats in the other groups in the ON condition (pairwise comparisons: $P = 0.0418$ for ADS vs. OLS, $P = 0.0012$ for ADS vs. control, and $P = 0.2110$ for OLS vs. control; Fig. 3 and Movies S1 and S2). By postlesion day 14, the performance of the rats in the ADS group was approximately at prelesion levels and significantly higher than that of rats in the other groups. The difference between the OLS group and the control group approached significance on day 14 (global comparison: $P = 0.0004$; pairwise comparisons: $P = 0.0284$ for ADS vs. OLS, $P < 0.0001$ for ADS vs. control, and $P = 0.0555$ for OLS vs. control). By postlesion day 21, performance in the ADS group remained high and statistically different from that of the control group. Performance was not significantly different in the ADS group between days 14 and 21 ($P = 0.576$). However, by day 21, the OLS group had improved further, so that the difference between the two groups was not significant (global comparison: $P = 0.0007$;

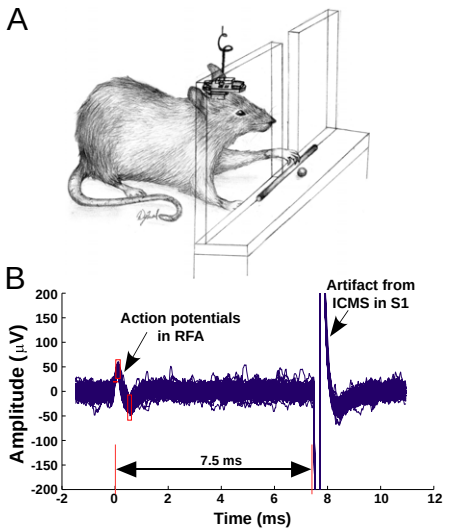

Fig. 2. ADS protocol. After injury to the CFA, a recording microelectrode was placed in the RFA, whereas a stimulating microelectrode was placed in the distal forelimb field of S1. A BMBI discriminated action potentials in the RFA, and after a 7.5-ms delay, it delivered a low-level electrical current pulse to S1 (13). (*A*) Sketch of a rat retrieving a food pellet with a BMBI attached to the skull. (*B*) Sample traces of recordings from the RFA showing action potentials and stimulus artifacts from an ICMS current delivered to S1. Time-amplitude window discriminators are indicated by red boxes. A total of 100 superimposed traces are shown.

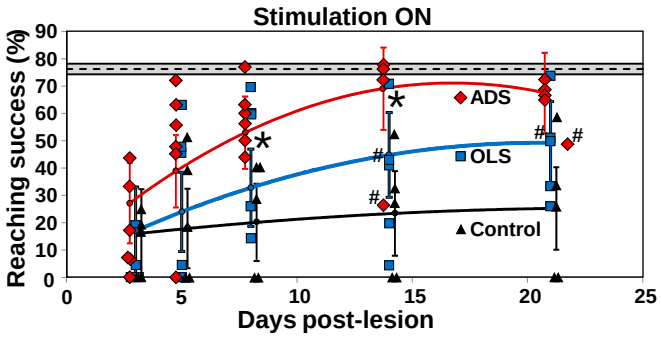

Fig. 3. Performance of rats on a skilled reaching task after injury to M1 (ON condition). The ADS group is shown in red, the OLS group is shown in blue, and the control group is shown in black. The dotted line indicates the average prelesion performance of all animals in the study. The bounded area indicates the 95% confidence interval. Regression lines are based on an LMM (43). Error bars represent 95% confidence intervals. *$P < 0.05$ (pairwise difference between the ADS and OLS groups). Because the statistical analysis was an intent-to-treat model, rats were included in the analysis even if the microdevice was no longer functional. Only one rat in the ADS group had a microdevice that was functional by postlesion day 28; thus, figures are presented through postlesion day 21 (*SI Results*). Diamonds, squares, and triangles represent individual animal data points. #, microdevice not functional (Tables S1 and S2).

pairwise comparisons: $P = 0.0891$ for ADS vs. OLS, $P = 0.0002$ for ADS vs. control, and $P = 0.0278$ for OLS vs. control). Although the mean performance of the ADS group was higher than that of the OLS group even in the OFF condition, differences were not statistically significant on any postlesion day (Fig. S2).

Immediate Effects Within Single Sessions. Rats in the ADS group often showed substantially improved performance within a single day's session when the microdevice was switched from the OFF to the ON condition. One particularly salient example can be seen in a video of a rat in the ADS group on postlesion day 8 (Movie S2). In the OFF condition, this rat made many attempts to reach through the opening in the Plexiglas but was rarely able to do so accurately. Large trajectory errors were made, and relatively few retrievals were completed successfully. Following completion of trials in the OFF condition, the microdevice was programmed to the ON state, a process that required 2–3 min. As soon as the microdevice was turned ON, the rat began to retrieve pellets with noticeably enhanced success. Movements tended to be slower and seemingly more deliberate, and fewer errors were made. A statistical analysis of the ADS group between the OFF and ON conditions revealed significantly better performance in the ON condition on postlesion day 3 ($P = 0.0003$), postlesion day 5 ($P = 0.0005$), and postlesion day 8 ($P = 0.0019$) and marginally better performance on postlesion day 14 ($P = 0.0666$). The same analysis for the OLS group revealed significantly worse performance in the ON condition on postlesion day 3 ($P = 0.0471$) and marginally worse performance on postlesion day 5 ($P = 0.0554$) and postlesion day 8 ($P = 0.0781$) (Fig. S3). These effects tended to dissipate over time, so that no differences were detected between OFF and ON conditions in either group by postlesion day 21. These within-day differences through postlesion day 8 suggest that the timing of the S1 stimulus pulse is critical. Behavioral performance was significantly better when the S1 stimulus pulse was delivered contingent upon an action potential in the RFA (i.e., in the ADS group).

Effects of ADS on Functional Connectivity. To explore possible neurophysiological mechanisms underlying the behavioral effects of the ADS treatment on postinjury motor performance, we performed post hoc analysis of spike events in the RFA that were discriminated in the 28 ms after each S1 stimulus pulse. This time window represented our imposed blanking period during which additional S1 stimulus pulses could not occur. Poststimulus spike histograms were compared with 28-ms periods chosen from data acquired in the OFF condition 7.5 ms after each RFA spike event. The results show that substantially more spikes in the RFA occurred following S1 stimulation in the ADS group, with peak activity occurring ~4–6 ms after the S1 stimulus pulse (Fig. 4*A*). Spike rates were nearly threefold higher averaged across the 28-ms period compared with a comparable period in the OFF condition. Spike rates in the OLS group were slightly lower than in the ADS group in the OFF condition but were significantly lower than in the ADS group in the ON condition. These data suggest that ADS substantially reinforced network interactions between S1 and the RFA, whereas OLS did not.

Subdividing the spike histograms by day reveals that enhanced spike activity in the ADS ON condition is evident even on the first day that the microdevice was activated (Fig. 4*B* and Fig. S4). There is also a trend toward further increases in spike discharge between the first (days 1 and 5) and second (days 8 and 14) weeks in the ADS group, corresponding to the time period when behavioral performance approached normal levels.

Whether behavioral performance and enhanced functional connectivity persist following the end of treatment cannot be addressed fully based on the current results (*SI Discussion*). However, it is noteworthy that there was a significant decrease in mean performance in the ADS group between postinjury days 21 and 28 (Fig. S5). During this time period, microelectrode-microdevice connection failures prevented normal operation of the microdevice in most of the ADS rats. This phenomenon of reduced behavioral performance after deactivation provides further

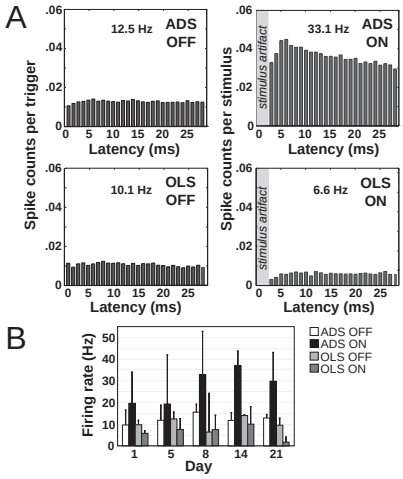

Fig. 4. Comparison of spike activity in the RFA in the ADS and OLS groups. Data represent spikes discriminated in the RFA over a 28-ms period. In the ON condition, the trigger for the data acquisition was the S1 stimulus pulse. In the OFF condition, the trigger for the data acquisition was 7.5 ms after a spike event in the RFA. (*A*) Composite posttrigger spiking histograms derived from neural recordings in the RFA compiled from days 1, 5, 8, 14, and 21 (±1 d). Histograms portray the mean spike counts per trigger event within each time bin (also Fig. S4). Spike counts were based on an average of over 22,000 trigger events per animal per day. Poststimulus firing rates were substantially higher in the ADS ON condition (33.1 Hz), compared with the ADS OFF (12.5 Hz), OLS ON (6.6 Hz), or OLS OFF (10.1 Hz) condition. (*B*) Average spike firing rates throughout the 28-ms window for each day. Error bars represent between-subject variation on each day (plus 1 SD). LMMs detected higher firing rates in the ADS group compared with the OLS group with stimulation ON ($P < 0.0001$). Firing rates did not differ statistically between groups in the OFF condition ($P > 0.05$). Posttrigger spiking histograms for each day are shown in Fig. S4.

support for the notion that the behavioral improvements were mediated by closed-loop operation. It also suggests that either a longer duration of operation (i.e., beyond 21 d) is required for persistent effects or that closed-loop stimulation enhances the rate, but not the extent, of recovery compared with OLS. Nonetheless, the present data provide persuasive evidence that targeted closed-loop stimulation approaches are feasible as brain repair strategies. Rapid behavioral recovery parallels the development of increased functional connectivity between spared somatosensory and motor regions of the cortex.

Discussion

This proof-of-concept study indicates that a closed-loop neuroprosthetic microdevice can enhance functional connectivity between distant cortical locations and generate rapid improvement in motor function after cortical injury, at least in rats with M1 damage. A closed-loop device with similar functionality induced neurophysiological changes when applied over a short distance within M1 of intact monkeys (15). More recently, spike-triggered stimulation was used to demonstrate increased potentiation between neurons in the sensorimotor cortex of rats. The spike-stimulation delay was important, because 5 ms resulted in robust increases, whereas 100 or 500 ms resulted in no potentiation (16). The present study demonstrates that the extension of the ADS approach to injured brains has demonstrable effects on recovery and establishes functional communication that is qualitatively different compared with uncorrelated stimulation. The current implementation of the system architecture, using a lightweight, battery-powered, wireless, miniaturized microdevice for spike-triggered intracortical microstimulation (ICMS), represents an important step in the process of developing implantable BMBIs for neural repair in clinical populations.

Differential Mechanisms Underlying the Effects of OLS and ADS on Behavioral Recovery. The mechanisms underlying the therapeutic effects of OLS and ADS after injury in the present model of TBI are still somewhat speculative. In the 1940s, Donald Hebb (17) postulated that "When one cell repeatedly assists in firing another, the axon of the first cell develops synaptic knobs… in contact with the soma of the second cell." This hypothesis has morphed into the modern maxim "Cells that fire together, wire together," a phrase made popular by neuroscientist, Carla Shatz (18). A large literature has grown from these initial hypotheses, and a neurophysiological phenomenon widely known as "Hebbian plasticity" has formed the basis for many neuroscientific models of learning and memory. Previous studies in intact primates and rodents using ADS or paired-pulse stimulation show the ability for such coactivation to alter output properties of cortical neurons (15, 16, 19). Presumably, the stimulation causes Hebbian-like plasticity to alter existing connectivity within a cortical area.

Although significant behavioral recovery occurred in both the ADS and OLS groups compared with control rats, the ADS group improved substantially more rapidly. Also, in the early postlesion period, the ADS group demonstrated a qualitatively different ON vs. OFF performance compared with the OLS group. These behavioral results alone suggest that different mechanisms underlie recovery in ADS and OLS groups. Although the results of ICMS on behavioral outcomes in animal models of brain injury have not been reported previously, several studies have examined the therapeutic effects of surface stimulation in either human stroke survivors or animal stroke models. For example, an invasive technology using epidural stimulation to provide low-level current pulses over uninjured cortical areas during the execution of rehabilitative training resulted in behavioral improvement in rodent and nonhuman primate models of cortical ischemic injury (20, 21). Although initial results in clinical stroke populations were promising, the therapeutic effect of open-loop epidural stimulation was not demonstrated in a randomized clinical trial (22). Nonetheless, noninvasive cortical stimulation approaches (transcranial magnetic stimulation and transcranial direct-current stimulation) continue to attract substantial interest due to positive results in small groups of stroke survivors (23).

Evidence to support specific mechanisms underlying the effects of open-loop electrical stimulation of the cortex on recovery is largely correlative but includes motor map reorganization, increased dendritic length and spine density, cell proliferation and cell migration in the subventricular zone, receptor subunit expression, activation of antiapoptotic cascades, increased neurotrophic factors, enhanced angiogenesis, and proliferation of inflammatory cells (20, 21, 24–28). Because the number of stimulus pulses was similar in the ADS and OLS groups in the present study, it is reasonable to conclude that if electrical stimulation promoted proliferative processes, the effects were the same in the two groups.

In addition, various OLS protocols produce alterations in synaptic efficacy. These data are particularly relevant because of the qualitative differences in functional connectivity observed between ADS and OLS groups. Long-term potentiation (LTP), an experimental phenomenon first discovered in the hippocampus of anesthetized rabbits over 40 y ago (29), is expressed in both excitatory and inhibitory synapses throughout the mammalian brain (30). Although many experimental protocols have been developed to optimize synaptic potentiation in various model systems, the sign and magnitude of synaptic potentiation are heavily dependent upon the frequency and pattern of stimulation (31, 32).

Despite comparable mean stimulation frequency between the two groups, the temporal structure of stimulus pulses differed between the ADS and OLS groups. Interstimulus intervals spanned approximately the same range, but the intrinsic temporal firing pattern observed in the ADS group resulted in a greater number of short interstimulus intervals (Fig. S6*A*). Thus, ADS stimulation occasionally consisted of stimulus pulses at higher frequency, somewhat analogous to theta-burst stimulation, in which train bursts of high-frequency pulses (e.g., four to eight pulses at 100–300 Hz) are delivered at about 6–7 Hz (i.e., within the theta-rhythm frequency). Theta-burst stimulation is often used to optimize generation of LTP, especially in the neocortex of awake animals, where LTP has traditionally been more difficult to generate (33). In a study in the neocortex of freely moving rats, theta-burst stimulation, using parameters similar to those used in the hippocampus, evoked LTP, but the effects required at least 5 d to develop and plateaued at about 15 d (34). In the present study, although enhanced, short-latency spike discharge was evident with ADS even on the first day of stimulation, the time course of the behavioral effects was remarkably similar to the slowly developing LTP found in the rat neocortex study.

Theta-burst timing protocols vary considerably depending upon the particular model system. However, a recent study in a mouse brain slice preparation in the dorsal striatum suggests that the optimal theta-burst patterns are those that best match intrinsic neural activity patterns (35). Further, "burstiness" was critical to inducing LTP. Simply reducing the interburst pause from 35 ms to 20 ms eliminated the induction of LTP. It is possible that our imposed 28-ms blanking period further contributed to the neurophysiological and behavioral effects. We propose that by using a closed-loop stimulation paradigm, the intrinsic stimulation patterns that optimally drive synaptic potentiation in the cortico-cortical pathways were used. (The feasibility of using optimal theta-burst parameters in an open-loop mode of stimulation is discussed in *SI Discussion*).

In summary, OLS and ADS may both contribute to behavioral recovery but by somewhat different mechanisms. Electrical stimulation, in general, is likely to modulate neuronal growth processes, leading to adaptive plasticity that could account for at least part of the behavioral improvement. In the closed-loop (ADS) condition, however, the intrinsic firing pattern drives synaptic

potentiation in a manner similar to that observed in theta-burst protocols. Although potentiation builds rapidly (within 1 d), we propose that chronic ADS results in a behaviorally relevant, functional connection between S1 and PM.

Future Applications of Closed-Loop Neuroprostheses for Treating Neurological Disorders. A closed-loop neuroprosthesis applying ADS across distant cortical areas is a vastly different approach to brain repair than has been achieved to date. Therapeutic closed-loop stimulation in the brain is still uncommon. However, analogous approaches are already being tested for epilepsy, and an expanded role for closed-loop systems for deep brain stimulation in Parkinson disease is now being considered (36, 37). Further, closed-loop approaches are under development in animal models of spinal cord injury (38, 39). Other investigators have proposed a closed-loop approach for a cognitive prosthesis that has shown promise in animal models (40). Other potential clinical applications based on the current model include stroke, focal TBI, and surgical resections. Finally, a variety of neurological syndromes that are thought to be related to disruption of cortical communication may be amenable to ADS. In the 1960s, Norman Geschwind identified several disorders collectively called "disconnection syndromes," revolutionizing the field of behavioral neurology (41). The consideration of closed-loop approaches to repair of cortical disconnection syndromes may open treatment options for a variety of conditions in which neural communication is disrupted, whether due to disease, injury, or idiopathic causes.

Materials and Methods

Animals. Adult, male Long–Evans hooded rats (n = 16, weight: 350–450 g; Harlan) were procured at 4 mo of age. Protocols for animal use were approved by the Kansas University Medical Center Institutional Animal Care and Use Committee and adhered to the *Guide for the Care and Use of Laboratory Animals* (42). Each rat was singly housed in a transparent cage and provided with food and water ad libitum. The room was kept on a 12-h:12-h light/dark cycle, and ambient temperature was maintained at 22 °C.

Rats were assigned to three groups: the ADS group, the OLS group, and the control group. Rats in all three groups received a CCI injury over the M1 forelimb area (5). Postmortem histological analysis confirmed that lesion size was comparable across groups (*SI Results*). The surgical procedures (e.g., burr holes, skull screws, dura resection) were identical in all three groups. Microelectrode implantation and microdevice attachment were identical in the ADS and OLS groups. In both the ADS and OLS groups, one single-shank microelectrode array was inserted into the S1 forelimb area. A second single-shank microelectrode array was inserted into the RFA (depths are provided in *SI Materials and Methods*). In the ADS group, stimulation in S1 was contingent upon spike activity in the RFA; that is, time-amplitude window discriminators determined when action potentials were recorded from the RFA microelectrode. Discrimination of an individual action potential triggered delivery of a brief pulse of electrical current to the microelectrode implanted in S1. In the OLS group, the stimulation was delivered arbitrarily at a frequency approximately the same as that in the ADS group but with the timing of stimulation uncorrelated with the discriminated action potentials (*SI Materials and Methods*). The wireless, battery-powered microdevice, mounted to the freely moving rat's skull, operated 24 h per day (Fig. 2*A* and Fig. S1).

CCI Procedure. In each rat, the skull over the CFA was removed while leaving the dura intact. A 3-mm diameter rod with a flat tip was placed into a commercial impactor device (Leica Microsystems), centered over the target location (*SI Materials and Methods*), and then lowered until the surface of the tip was in contact with the dura, as indicated by an audible signal triggered by a feedback sensor. The rod was then retracted and armed. An impact was delivered with an excursion of 2 mm below the surface of the dura. This protocol leads to reproducible lesions that damage all cortical layers within the CFA with minimal superficial damage to underlying white matter tracts and limited or no damage to adjacent cortical areas (5).

Microdevice Programming. ***ADS programming.*** To determine discrimination parameters for ADS, the channel with the best signal-to-noise ratio was chosen. This same channel was later used during microdevice operation to determine spike events that triggered stimulation. Using a custom MATLAB (MathWorks) script, action potentials were discriminated offline by thresholding and two user-adjustable time-amplitude windows, with the intent of maximizing discrimination of observed spikes while minimizing noise and/or stimulus artifacts. Stimulation parameters were set to deliver a 60-μA, 192-μs, pseudobiphasic current pulse with a 7.5-ms delay following spike discrimination (Fig. 2*B*). A blanking interval following each spike discrimination prevented additional stimulus pulses for 28 ms. The spike discrimination, timing, and stimulation parameters were then uploaded to the microdevice for online spike discrimination. Thus, during device operation in the ADS group, each discriminated spike in PM triggered a stimulation pulse in S1, constrained by the blanking interval.

The 7.5-ms delay was based on previous studies of the effective delay within local networks, analysis of spike-stimulus delays in pilot data, as well as constraints in the current microdevice architecture. The 28-ms blanking interval was also based on analysis of spike-stimulus delays in pilot data and was set to reduce the possibility of producing a positive-feedback loop, in which S1 stimulation might drive action potentials in PM, retriggering stimulation of S1.
OLS programming. Stimulation parameters were the same in the OLS group as for the ADS group. However, the stimulation was not contingent upon recorded neural activity. Instead, the stimulation was set to occur arbitrarily with interstimulus intervals ranging from 35 to 200 ms (randomized equally across the range), closely approximating the stimulus rate for the ADS group (*SI Materials and Methods*, *SI Results*, and Fig. S6*A*).
Signal monitoring and maintenance. The neural activity and stimulation rates were monitored daily throughout the study via a wireless connection. The microdevice ran continuously, delivering ADS or OLS 24 h a day during the experiment, except for brief periods required for behavioral assessment, changing the battery, and adjusting the window discriminator parameters.

Bandpass-filtered neural data (~500 Hz to 5 kHz) were recorded at ~35.7 kHz per channel from either one or four channels (wireless or wired connection, respectively) during all signal monitoring and behavioral trials using LabVIEW software (National Instruments). In addition, all animals had multiple sessions during which data were recorded during home cage behavior. The raw signal recording duration of any single monitoring period was software-limited to ~45 min, but the stimulus trigger signal could be recorded for up to 24 h. The neural signal data were converted from a LabVIEW file to a text file and analyzed using custom MATLAB software.

Behavioral Training and Assessment. ***Skilled reaching task.*** Each rat was tested in a 30-cm × 30-cm × 52-cm Plexiglas reaching chamber. For each trial, a single food pellet (45 mg; Bioserv) was placed into a shallow well 2 cm from the front wall on an external shelf positioned 3 cm from the bottom of the chamber. The rat was required to reach through a narrow slot to retrieve the pellet with its forepaw (Fig. 2*A*). After forelimb preference was determined, a removable Plexiglas wall was used to force the animal to use only the preferred forelimb (5). Trials were recorded with a digital camcorder for playback and analysis. The percentage of success was measured as the percentage of trials in which the rat grasped, retrieved, and brought the pellet to the mouth (60 trials per day). Before entry into the remainder of the study, the rat was required to reach and retrieve food pellets above 70% success for 3 consecutive days. Following the injury (see below), behavioral probing sessions were conducted on postlesion days 3, 5, 8, 14, 21, and 28. Testing on postlesion days 1 and 2 was not practical due to the effects of surgical recovery and postsurgical analgesics on behavioral performance. Probing sessions consisted of 20 trials with the microdevice stimulation function turned OFF and then 20 trials with the microdevice stimulation function turned ON.
Foot-fault task. Rats were also assessed on a foot-fault task to determine the effects of the injury on a locomotion task. In general, although there was an effect of the injury on this task on postlesion day 3, no lesion effects were observed on subsequent days. Also, there were no differences between groups at any time points. This result was not unexpected, because the foot-fault task is less sensitive, and spontaneous recovery is common with lesions restricted to the forelimb motor cortex.

Statistical Analysis of Behavioral Performance. Initially, animals were randomly assigned to an ADS (n = 6) or control (n = 5) group. A subsequent OLS group (n = 5) was studied after group randomization. This was necessary to use neurophysiological data from the ADS group to determine the stimulation protocol for the OLS group.

Linear mixed models (LMMs) (43) were generated via restricted maximum likelihood estimation using SAS version 9.2 PROC GLIMMIX (SAS Institute, Inc.) to model performance on the skilled reaching task for each animal over time. Results are presented to mirror a series of one-way ANOVA models because the LMM provides analogous results. For animals in the ADS and

OLS groups, the difference between the OFF and ON conditions was studied as an outcome. Models included fixed effects for treatment group, time, and their interaction.

Time was treated as a continuous measure to generate estimates of a polynomial relationship for recovery profiles in each treatment group over time up to a (treatment group-specific) quadratic relationship. Animal-specific effects were introduced by allowing for random intercepts in these models; thus, the models allowed for estimation of normally distributed error terms both for between- and within-animal effects. Backward elimination was used to determine the functional form of these relationships with F test P values <0.05 for effects to remain in the models. All lower ordered terms were retained in models in the presence of higher level interaction effects, regardless of statistical significance. Models were evaluated by visual inspection of observed vs. predicted values for each animal to assess model fit, observed vs. residuals plots to assess constant variance assumptions, and histograms of the residuals and quantile-quantile plots to assess the assumption of normally distributed random effects. Residuals included both those for the random intercept coefficients (for between-animal error terms) and overall residuals (for within-animal error terms).

Linear contrasts of model estimates were used to test for treatment group differences on postlesion days 3, 5, 8, 14, 21, and 28 using F tests, with day 28 serving as the a priori time point of interest for the comparison of ADS vs. OLS. Other pairwise comparisons at each time point were also tested (*SI Materials and Methods*, *Protocol Deviations*). Given the single, a priori primary comparison, no further adjustments for multiple comparisons were made. Linear contrasts were used to generate 95% confidence intervals for each treatment group for those specific days and, within the ADS and OLS groups, to test for differences in the OFF vs. ON conditions. Two-sided P values were used for presentation of results.

ACKNOWLEDGMENTS. The authors thank Andrea Pack and Alexandra Brown for technical assistance, Cam Teskey for invaluable comments on the discussion, and Casey Wood for artistic contributions. This research was funded by the Department of Defense Traumatic Brain Injury-Investigator-Initiated Research Award Program under Awards W81XWH-10-1-0741/0742 (to P.M. and R.J.N.) and the American Heart Association under Award 09BGIA2280495 (to P.M.). The fabrication costs for the chip in the microdevice were generously supported by the Advanced Platform Technology Center—A Veterans Affairs Research Center of Excellence (Cleveland, OH).

1. Vicente R, Gollo LL, Mirasso CR, Fischer I, Pipa G (2008) Dynamical relaying can yield zero time lag neuronal synchrony despite long conduction delays. *Proc Natl Acad Sci USA* 105(44):17157–17162.
2. Carter AR, Shulman GL, Corbetta M (2012) Why use a connectivity-based approach to study stroke and recovery of function? *Neuroimage* 62(4):2271–2280.
3. Nudo RJ (2011) Neural bases of recovery after brain injury. *J Commun Disord* 44(5): 515–520.
4. Webster BR, Celnik PA, Cohen LG (2006) Noninvasive brain stimulation in stroke rehabilitation. *NeuroRx* 3(4):474–481.
5. Nishibe M, Barbay S, Guggenmos D, Nudo RJ (2010) Reorganization of motor cortex after controlled cortical impact in rats and implications for functional recovery. *J Neurotrauma* 27(12):2221–2232.
6. Friel KM, et al. (2005) Dissociation of sensorimotor deficits after rostral versus caudal lesions in the primary motor cortex hand representation. *J Neurophysiol* 94(2): 1312–1324.
7. Conner JM, Chiba AA, Tuszynski MH (2005) The basal forebrain cholinergic system is essential for cortical plasticity and functional recovery following brain injury. *Neuron* 46(2):173–179.
8. Nudo RJ, Frost SB (2009) The evolution of motor cortex and motor systems. *Evolutionary Neuroscience*, ed Kaas JH (Academic, Oxford), pp 727–756.
9. Rouiller EM, Moret V, Liang F (1993) Comparison of the connectional properties of the two forelimb areas of the rat sensorimotor cortex: Support for the presence of a premotor or supplementary motor cortical area. *Somatosens Mot Res* 10(3):269–289.
10. Dum RP, Strick PL (2002) Motor areas in the frontal lobe of the primate. *Physiol Behav* 77(4-5):677–682.
11. Dancause N, et al. (2005) Extensive cortical rewiring after brain injury. *J Neurosci* 25(44):10167–10179.
12. Fang PC, Stepniewska I, Kaas JH (2005) Ipsilateral cortical connections of motor, premotor, frontal eye, and posterior parietal fields in a prosimian primate, *Otolemur garnetti*. *J Comp Neurol* 490(3):305–333.
13. Azin M, Guggenmos DJ, Barbay S, Nudo RJ, Mohseni P (2011) A miniaturized system for spike-triggered intracortical microstimulation in an ambulatory rat. *IEEE Trans Biomed Eng* 58(9):2589–2597.
14. Azin M, Guggenmos DJ, Barbay S, Nudo RJ, Mohseni P (2011) A battery-powered activity-dependent intracortical microstimulation IC for brain-machine-brain interface. *IEEE J Solid-State Circuits* 46(4):731–745.
15. Jackson A, Mavoori J, Fetz EE (2006) Long-term motor cortex plasticity induced by an electronic neural implant. *Nature* 444(7115):56–60.
16. Rebesco JM, Miller LE (2011) Stimulus-driven changes in sensorimotor behavior and neuronal functional connectivity application to brain-machine interfaces and neurorehabilitation. *Prog Brain Res* 192:83–102.
17. Hebb DO (1949) *The Organization of Behavior* (Wiley, New York).
18. Shatz CJ (1992) The developing brain. *Sci Am* 267(3):60–67.
19. Rebesco JM, Stevenson IH, Körding KP, Solla SA, Miller LE (2010) Rewiring neural interactions by micro-stimulation. *Front Syst Neurosci* 4:39.
20. Adkins-Muir DL, Jones TA (2003) Cortical electrical stimulation combined with rehabilitative training: Enhanced functional recovery and dendritic plasticity following focal cortical ischemia in rats. *Neurol Res* 25(8):780–788.
21. Plautz EJ, et al. (2003) Post-infarct cortical plasticity and behavioral recovery using concurrent cortical stimulation and rehabilitative training: A feasibility study in primates. *Neurol Res* 25(8):801–810.
22. Plow EB, Carey JR, Nudo RJ, Pascual-Leone A (2009) Invasive cortical stimulation to promote recovery of function after stroke: A critical appraisal. *Stroke* 40(5): 1926–1931.
23. Perez MA, Cohen LG (2009) The corticospinal system and transcranial magnetic stimulation in stroke. *Top Stroke Rehabil* 16(4):254–269.
24. Adkins DL, Hsu JE, Jones TA (2008) Motor cortical stimulation promotes synaptic plasticity and behavioral improvements following sensorimotor cortex lesions. *Exp Neurol* 212(1):14–28.
25. Baba T, et al. (2009) Electrical stimulation of the cerebral cortex exerts antiapoptotic, angiogenic, and anti-inflammatory effects in ischemic stroke rats through phosphoinositide 3-kinase/Akt signaling pathway. *Stroke* 40(11):e598–e605.
26. Henderson AK, Pittman QJ, Teskey GC (2012) High frequency stimulation alters motor maps, impairs skilled reaching performance and is accompanied by an upregulation of specific GABA, glutamate and NMDA receptor subunits. *Neuroscience* 215:98–113.
27. Jahanshahi A, et al. (2013) Electrical stimulation of the motor cortex enhances progenitor cell migration in the adult rat brain. *Exp Brain Res* 231(2):165–177.
28. Edwardson MA, Lucas TH, Carey JR, Fetz EE (2013) New modalities of brain stimulation for stroke rehabilitation. *Exp Brain Res* 224(3):335–358.
29. Bliss TV, Lomo T (1973) Long-lasting potentiation of synaptic transmission in the dentate area of the anaesthetized rabbit following stimulation of the perforant path. *J Physiol* 232(2):331–356.
30. Malenka RC, Bear MF (2004) LTP and LTD: An embarrassment of riches. *Neuron* 44(1): 5–21.
31. Feldman DE (2009) Synaptic mechanisms for plasticity in neocortex. *Annu Rev Neurosci* 32:33–55.
32. Feldman DE (2012) The spike-timing dependence of plasticity. *Neuron* 75(4):556–571.
33. Trepel C, Racine RJ (1998) Long-term potentiation in the neocortex of the adult, freely moving rat. *Cereb Cortex* 8(8):719–729.
34. Racine RJ, Chapman CA, Trepel C, Teskey GC, Milgram NW (1995) Post-activation potentiation in the neocortex. IV. Multiple sessions required for induction of long-term potentiation in the chronic preparation. *Brain Res* 702(1-2):87–93.
35. Hawes SL, Gillani F, Evans RC, Benkert EA, Blackwell KT (2013) Sensitivity to theta-burst timing permits LTP in dorsal striatal adult brain slice. *J Neurophysiol* 110(9): 2027–2036.
36. Skarpaas TL, Morrell MJ (2009) Intracranial stimulation therapy for epilepsy. *Neurotherapeutics* 6(2):238–243.
37. Santos FJ, Costa RM, Tecuapetla F (2011) Stimulation on demand: Closing the loop on deep brain stimulation. *Neuron* 72(2):197–198.
38. Jackson A, Zimmermann JB (2012) Neural interfaces for the brain and spinal cord—Restoring motor function. *Nat Rev Neurol* 8(12):690–699.
39. Nishimura Y, Perlmutter SI, Fetz EE (2013) Restoration of upper limb movement via artificial corticospinal and musculospinal connections in a monkey with spinal cord injury. *Front Neural Circuits* 7:57.
40. Berger TW, et al. (2012) A hippocampal cognitive prosthesis: Multi-input, multi-output nonlinear modeling and VLSI implementation. *IEEE Trans Neural Syst Rehabil Eng* 20(2):198–211.
41. Catani M, Mesulam M (2008) What is a disconnection syndrome? *Cortex* 44(8): 911–913.
42. Committee for the Update of the Guide for the Care and Use of Laboratory Animals (2011) *Guide for the Care and Use of Laboratory Animals* (The National Academies Press, Washington, DC).
43. McCulloch CE, Searle SR (2001) *Generalized, Linear, and Mixed Models* (Wiley, New York).

Supporting Information

Guggenmos et al. 10.1073/pnas.1316885110

SI Materials and Methods

Targeting Sites for Injury and Microelectrode Implantation. Before creating the controlled cortical impact (CCI) injury (all animals) and implanting the microdevice [activity-dependent stimulation (ADS) and open-loop stimulation (OLS) groups], target locations were identified using stereotaxic coordinates and neurophysiological criteria in each of the animals in the ADS, OLS, and control groups. Surgical procedures were identical in the control group as the scalp was incised, burr holes were made at corresponding locations, and the dura was resected. However, no microelectrodes were implanted and no microdevice was attached.

Rostral forelimb area. First, a burr hole was made in the skull over the general location of the rostral forelimb area (RFA) based on stereotaxic coordinates [anteroposterior (AP), +3.5; mediolateral (ML), +2.5]. Borders between the RFA and surrounding representations were identified using intracortical microstimulation (ICMS) techniques (1). For this purpose, a single-shank, 16-channel Michigan probe (NeuroNexus Technologies) was inserted into the burr hole to a depth of 1,700 μm and ICMS currents were delivered. Stimulation pulses were generated through a constant-current stimulus isolation unit, providing a 40-ms train of thirteen 200-μs monophasic cathodal pulses delivered at 350 Hz at the rate of one train per second. The applied current was increased until a movement was observed or until the current level reached 100 μA. Movements about the shoulder, elbow, wrist, and digits were defined as forelimb sites, and thus contained within the RFA. The single-shank electrode was then removed.

Primary somatosensory cortex forepaw area. A second burr hole was made in the skull over the general location of the primary somatosensory cortex (S1) forelimb area (AP, −1.25; ML, +4.25). Receptive fields confined to the forepaw were identified using multiunit neural recordings. For this purpose, a single-shank, 16-channel Michigan microelectrode (NeuroNexus Technologies) was lowered into S1 so that microelectrode sites spanned cortical layers III–IV. Using commercial equipment (Tucker–Davis Technologies), neural activity was amplified, digitized, filtered, played through a loudspeaker, and displayed on a computer monitor. Receptive fields were defined by the extent of the skin surface over which neural activity could be evoked by light touch and/or palpation. The S1 distal forepaw area was defined by sites at which the receptive fields were relatively small and confined to the distal forelimb. Then, the microelectrode used for receptive field recording was removed.

Caudal forelimb area. A third burr hole was made over the caudal forelimb area (CFA), the target of the lesion. Based on a large number of previous mapping studies (1–3), stereotaxic coordinates are reliable for estimating the center of the CFA, and thus the center for the impactor tip (AP, +0.5; ML, +3.5). This allowed the dura to remain intact before the CCI injury.

CCI. Following creation of the burr hole over the CFA, a 3-mm diameter rod with a flat tip was placed into a commercial impactor device (Leica Microsystems), centered over the target location, and then lowered until the surface of the tip was in contact with the dura, indicated by an audible signal triggered by a feedback sensor. The rod was then retracted and armed. An impact was delivered at 1.5 m/s with 100 ms of dwell time and an indentation depth of 2 mm below the surface of the dura. This protocol leads to reproducible lesions that damage all cortical layers within the CFA with minimal superficial damage to underlying white matter tracts and limited or no damage to adjacent cortical areas (2).

Microdevice Procedures. ***Microdevice implantation.*** Following the impact, holes for skull screws and an anchoring rod were created using a small drill bit. Skull screws were implanted into the parietal bones, and an anchoring rod was implanted into the intraparietal bone. The screws and rod were further secured with dental acrylic (all animals). In both the ADS and OLS groups, a hybrid, 16-channel, single-shank, chronic Michigan microelectrode, optimized for recording (typical impedance of 1–1.2 MΩ), was inserted into the RFA using a micropositioner to a depth of 1,700 μm (recording sites located approximately from 1,500 to 1,700 μm below cortical surface) to place it approximately in cortical layer V. The shanks of the microelectrodes were 15 μm thick, and the width was ∼100 μm wide at the cortical surface, tapering to 33 μm wide at the deepest point. The probe and burr hole opening were sealed with a silicone polymer (Kwik-Cast; World Precision Instruments). The base of the probe connector was lowered onto the dental acrylic and fixed into place. An activated, 16-channel, single-shank, chronic Michigan probe optimized for stimulation (typical impedance of 600–800 kΩ preactivation and 70–100 kΩ postactivation) was inserted into the S1 forepaw field at a depth of 1,700 μm, with stimulation sites located roughly 800–1200 μm (approximately layers III–IV) below the cortical surface and fixed in place in the same manner. Any remaining exposed areas were covered with the silicone polymer before suturing the incision. The microdevice was then affixed to the threaded rod with stainless-steel nuts and spacers, and its connectors were plugged into those of the appropriate electrodes (Fig. S1). The animal was then given postoperative analgesics (buprenorphine, 0.6 mg/kg s.c.) and monitored until recovery.

Technical aspects of the microdevice have been described previously (4, 5). In short, the microdevice was able to record autonomously from up to four of the 16 channels on the Michigan probe located in the RFA; to amplify, digitize, and filter the neural signals; and to use a user-programmable spike discrimination algorithm to trigger delivery of ICMS current pulses to up to four of the 16 channels on the Michigan probe implanted in the S1 distal forepaw area. Because connections between distant cortical areas are commonly reciprocal, enhanced communication theoretically could be established by ADS in either direction. In the present study, individual spikes were detected in premotor cortex (PM) and subsequent stimulation was delivered to S1 after a brief delay. The main rationale for the direction of stimulation in this study is that we suspected that stimulation of PM during movement would be disruptive.

Two to four hours following implantation, the microdevice was activated by insertion of a 6.8-mm, 1.55-V coin battery with a capacity of 26 milliamp hours. The microdevice was then connected to a personal computer through a flexible, multiconductor cable and a custom controller board for programming and signal monitoring. Neural activity recorded in the RFA during the next few hours was used in determining the initial time-amplitude window discriminator parameters.

In considering the optimal delay for long-range corticocortical interfaces, it is important to note that a simple consideration of the normal transmission across the brain based on axonal conduction time is not necessarily the only guiding principle. Despite axonal conduction delays in corticocortical fibers of tens of milliseconds, distant regions demonstrate synchronous neuronal discharges that oscillate over time. Large ensembles of neurons within the network, including neurons in both cortical and subcortical structures, may underlie synchronous discharges (6). Thus, it is currently unknown whether similar effects could be

elicited with longer or shorter delay parameters, or whether it matters which region leads the other.

Microdevice reprogramming and replacement. During monitoring, if the observed raw waveforms showed inconsistencies with the discriminated spikes due to slight changes in waveform shape or electrode noise level, the microdevice was operated in the wired mode, the stimulation was turned OFF, and the activity was reprocessed through the spike discrimination software. To maximize spike discrimination, the threshold and/or discrimination windows were then slightly adjusted to compensate for discrimination inconsistencies. If no spikes were observed, the remaining channels were monitored. If there was neural activity on one or more of the remaining channels, the stimulation trigger was moved to the most active channel. In practice, this minor alteration of spike discrimination parameters and channel switching generally was only needed during the first few days after injury/microdevice activation.

If no activity was detected on any of the four channels, the microdevice was removed and the electrodes were tested with off-the-shelf components (Tucker–Davis Technologies). If the electrodes were still functional, a new microdevice was typically attached to the animal and reprogrammed as above (Table S1). However, due to the scarcity of the microdevices, if behavioral performance had already improved to near-normal levels, the microdevice was not replaced (ADS group: day 28, $n = 2$; OLS group: day 14, $n = 1$ and day 28, $n = 1$; Table S2). The primary reason that microdevices became nonfunctional was due to mechanical failure of the flexible ribbon cable or its attachment points. If the microdevice remained nonfunctional, the animal continued to be tested in the study because an intent-to-treat statistical model was used for analysis.

Histological Examination of Lesion. After an overdose of Beuthanasia (1–2 mL), animals were transcardially perfused using 3% (wt/vol) paraformaldehyde. The brains were removed and divided into right and left hemispheres. The tissue was then post-fixed in a 30% (vol/vol) glycerol solution. A sliding microtome was used to create a series of 50-μm thick frozen sections cut tangentially through the cortex. Every other section was stained with cytochrome oxidase and counterstained with cresyl violet. Sections were mounted to slides, dehydrated, and cover-slipped.

Images of cortical sections and a scale bar were obtained with a digital camera with a macro lens. The digital photos were imported into Photoshop (Adobe Systems, Inc.), and scaling was adjusted appropriately. For each section, the border of the lesion was estimated by superimposing a mirror image of the corresponding section from the intact hemisphere and then traced (2, 7). Lesion area was then calculated for each section, and total volume was computed for each subject using a cylinder rule (7). One subject died before the completion of the study (ADS group); thus, the histological material was not suitable for quantitative comparison.

Lesion sizes were compared first between groups using a one-way ANOVA. Model assumptions were evaluated with a residual histogram, quantile-quantile plot, residual vs. predicted plot, and box plots. These diagnostics suggested that model assumptions for the one-way ANOVA were not met. Because a log transformation failed to resolve this issue, an exact Kruskal–Wallis test was used instead. Descriptive statistics are presented using the original scale.

Statistical Methods. Three repeated measures were collected for each animal; thus, a linear mixed model (LMM) was used to estimate the average prelesion level. LMMs have been well established in the statistical and biomedical sciences literature for the analyses of data such as these, and they are more appropriate for this repeated-measures experimental design, as well as the typical nonlinear pattern of behavioral recovery (8). Treatment group differences were tested using an F test. Model assessment followed the approach described in *Materials and Methods*.

Post Hoc Neurophysiological Analysis. ***Data collection.*** For each of the ADS and OLS animals, neurophysiological data were recorded from the microelectrode in the RFA either via the wireless link during microdevice monitoring or via the wired link during behavioral testing. All data were then imported into MATLAB (MathWorks) for further analysis. Because neural recordings were similar in the wireless and wired modes, data in the two modes were pooled. The dataset comprised ~30 min of neurophysiological recordings for each animal per condition per day, and was thus adequate to provide a representative sample. Neurophysiological data analysis was restricted to days 1, 5, 8, 14, and 21 (±1 d), because these days contained a sufficient amount of data in both ON and OFF conditions. All available data recorded on a particular day were used in the analysis.

A MATLAB script first identified ON and OFF sessions based on the presence or absence of stimulus artifacts. Then, for ON sessions, (*i*) the time stamps of individual stimulation pulses were determined (signal passed through negative and positive limits) and (*ii*) the time stamps of neural spikes discriminated during the 28-ms period following each stimulus pulse were determined and used for further analysis. This period represented the imposed blanking period during which no additional stimulation could occur, and thus was uncontaminated with additional stimulus pulses. For OFF sessions, time stamps of neural spikes discriminated throughout the session were determined and used for further analysis. Spike discrimination was performed using the same time-amplitude window parameters used by the microdevice during the experimental period.

Stimulation rates. Stimulation rates were determined to provide evidence that the ADS and OLS groups received comparable numbers of stimulus pulses. For each animal on each day of recording, stimulation rate was calculated by dividing the total number of stimulus pulses (indicated by each stimulus artifact) by the total session length in seconds. An LMM was used to assess the stimulation rate as described previously for the statistical analysis of the behavioral performance.

Interstimulus intervals. Interstimulus intervals were calculated for the ADS group to determine the range of intervals to be programmed into the microdevice for OLS stimulation. Subsequently, interstimulus intervals were also calculated for the OLS group to verify that the programmed parameters were implemented accurately and reliably. The interstimulus interval was calculated by subtracting the time stamps of each stimulus pulse from the immediately preceding stimulus pulse. All interstimulus intervals for all animals on days 1–21 were pooled within each group, and a composite histogram of interstimulus intervals up to 500 ms was created with a bin resolution of 10 ms. The bins were then normalized to the total length of all sessions within each day.

Interspike intervals. Interspike intervals were determined to examine the pattern of spike activity in the RFA throughout the course of the study. For each of the four conditions (ADS ON, ADS OFF, OLS ON, and OLS OFF), the intervals between spikes were calculated for every spike recorded for all animals on all behavioral testing days on which the device was functional. For each condition, data were pooled and a composite histogram of intervals up to 28 ms was created with a bin resolution of 1 ms. In each condition, spikes were normalized to the total number of spikes detected.

Poststimulus spike firing rates. Poststimulus spike firing rate histograms were derived to determine if the neural spikes in the RFA evoked from stimulation in S1 were altered by ADS or OLS. In the ADS and OLS ON conditions, we limited the dataset to the 28 ms following each stimulus pulse. Due to our imposed blanking period, this 28-ms window was uncontaminated with additional stimulus pulses. On average, the sample dataset used for poststimulus spike firing rate analysis represented over 22,000 stimulus pulses per animal per day. Due to the presence of stimulus artifact, it was not possible to discriminate spikes reliably within

the first 2 ms immediately following the stimulus pulse. Histograms of the 28-ms period following the stimulus pulse were generated for each animal on each behavioral testing day and normalized to the total number of stimulus pulses (i.e., total number of 28-ms periods).

In both the ADS and OLS OFF conditions, the data were processed into analogous 28-ms segments except that an initial spike (in RFA) was used to trigger the onset of the analysis. Subsequent spikes were discriminated after a 7.5-ms delay (similar to the spike-stimulus delay in the ADS ON condition) for the next 28 ms. After an artificial blanking period of 28 ms, the subsequent spike was used to trigger the next spike analysis period. Histograms were referenced to the trigger spike (+7.5 ms) and normalized to the total number of trigger events (i.e., total number of 28-ms periods). Composite histograms were also created to collapse data across various time domains.

For each condition, firing rates (in hertz) were calculated by summing the normalized bin values across the 28-ms window and then dividing by 28 ms. An LMM was used to assess the spike firing rates as described previously for the statistical analysis of the behavioral performance, with the addition of log transformations to stabilize the variance as indicated by model diagnostics. A constant was added for the ON minus OFF outcomes to ensure nonnegative values before log transformation.

Protocol Deviations. The primary between-group comparison for the skilled reaching task outcome was for tasks performed while the stimulation was being delivered (ON condition). However, because the microdevice was found to be nonfunctional in some animals on particular testing days (Tables S1 and S2), an intent-to-treat approach was used. These time points were excluded for the model in animals where the outcome was the difference between the stimulation ON and OFF conditions. For animals that died before day 28 (one animal in the ADS group), all available time points were included in the LMMs. It is important to note that use of the intent-to-treat approach resulted in a conservative estimate of treatment effect. If data from animals on days on which the microdevice was nonfunctional were excluded from the analysis, the effects of ADS would be greater.

SI Results

Behavioral Performance. ***General observations.*** No evidence of increased morbidity was observed in the animals, because all were similarly active and maintained normal eating and drinking patterns. Also, because all three groups performed equally well at a foot-fault task after day 3, there was no evidence for increased morbidity as a function of group assignment.

Prelesion skilled reaching task performance. No between-group (ADS, OLS, or control) differences were detected in prelesion skilled reaching task performance ($P = 0.7830$). A reduced model excluding treatment group indicated the mean prelesion performance to be 0.76 (95% confidence interval: 0.74–0.78). Model diagnostics indicated an adequate fit for this reduced model.

Skilled reaching task performance: Stimulation ON. No significant differences were detected ($P = 0.9715$) for ADS vs. OLS pairwise comparison on postlesion day 28, our a priori primary comparison (the test of no differences across all three groups at this time point was also not rejected with $P = 0.2379$). This was not surprising, because only one ADS animal had a functional microdevice on day 28. As can be seen in Fig. S5, there was a significant reduction in mean performance in the ADS group between days 21 and 28 ($P = 0.0011$), so that the ADS group was more comparable to the OLS group (but still substantially better than the control group). This reinforces the notion that ADS was necessary for maintenance of performance gains. Given the issues with nonfunctional devices on postlesion day 28, we proceeded to examine secondary comparisons on the remaining days. Higher skilled reaching task scores for group comparisons were detected across groups on postlesion day 8 ($P = 0.0044$; $P = 0.0418$ for ADS vs. OLS, $P = 0.0012$ for ADS vs. control, and $P = 0.2110$ for OLS vs. control), day 14 ($P = 0.0004$; $P = 0.0284$ for ADS vs. OLS, $P < 0.0001$ for ADS vs. control, and $P = 0.0555$ for OLS vs. control), and day 21 ($P = 0.0007$; $P = 0.0891$ for ADS vs. OLS, $P = 0.0002$ for ADS vs. control, and $P = 0.0278$ for OLS vs. control), but not on day 3 or day 5. Model diagnostics indicated an adequate fit for this model for the stimulation ON condition.

Because an intent-to-treat model was used for the statistical design, the performance of the ADS group on days 14 and 21 may have been attenuated somewhat due to a rat with a nonfunctioning device, potentially resulting in the nonsignificant difference with the OLS group on day 21. However, the difference in performance (ON condition) between days 14 and 21 was not significant in the ADS group ($P = 0.576$) but approached significance in the OLS group ($P = 0.0898$). Thus, the ADS group had achieved maximal performance by day 14, and the performance of the OLS group approached the range of the ADS group at a later time point. In general, rats in both the ADS and OLS groups improved, but the rats in the ADS group did so at a substantially more rapid rate. Rats in the OLS group performed at a level of performance intermediate between the control and ADS groups until day 21, when their performance began to approach that of the ADS group.

Skilled reaching task performance: Stimulation OFF. Increased skilled reaching task scores were detected across groups on postlesion day 8 ($P = 0.0229$), day 14 ($P = 0.0014$), and day 21 ($P = 0.0010$) but not on day 3 ($P = 0.6504$), day 5 ($P = 0.2579$), or day 28 ($P = 0.1358$). Pairwise comparisons within these time points were as follows: $P = 0.3845$ for ADS vs. OLS, $P = 0.0069$ for ADS vs. control, and $P = 0.0686$ for OLS vs. control for day 8; $P = 0.1246$ for ADS vs. OLS, $P = 0.0003$ for ADS vs. control, and $P = 0.0316$ for OLS vs. control for day 14; and $P = 0.1571$ for ADS vs. OLS, $P = 0.0002$ for ADS vs. control, and $P = 0.0186$ for OLS vs. control for day 21. Model diagnostics indicated an adequate fit for this model for the stimulation OFF condition (Fig. S2).

Difference in skilled reaching task performance for stimulation OFF vs. ON. Overall, skilled reaching task scores were higher for the stimulation ON (vs. OFF) condition in the ADS group on postlesion day 3 ($P = 0.0003$), day 5 ($P = 0.0005$), and day 8 ($P = 0.0019$), and they were marginally higher ($P = 0.0666$) on day 14 (Fig. S4). The same analysis for the OLS group revealed significantly worse performance in the ON condition on postlesion day 3 ($P = 0.0471$) and marginally worse performance on postlesion day 5 ($P = 0.0554$) and day 8 ($P = 0.0781$). This effect tended to dissipate over time, so that no differences were detected between OFF and ON conditions in either group by postlesion day 21. Model diagnostics indicated an adequate fit for this reduced model (Fig. S3).

Neurophysiological Data. ***Interstimulus intervals.*** As shown in Fig. S6*A*, the interstimulus intervals used for the OLS group comprised a comparable range compared with the ADS group. There was, however, a bias toward shorter interstimulus intervals in the ADS group, whereas the OLS intervals were equal across the range due to microdevice programming constraints.

Stimulation rates. The LMM detected statistical differences between the groups ($P = 0.0395$), but these differences represented a qualitative interaction (i.e., stimulation rates increased slightly for the ADS group and decreased slightly for the OLS group, with their trajectories crossing at approximately 1.5 wk). The overall mean stimulation rates of the ADS and OLS groups were quite similar at 8.26 Hz (SD = 3.86 Hz) and 8.18 Hz (SD = 1.42 Hz), respectively, which indicated similar amounts of stimulation were delivered to S1 in the ADS and OLS groups (Fig. S6*B*).

Interspike intervals. The distribution of interspike intervals was similar in the four conditions, with short interspike intervals (<10 ms) comprising a large proportion of the data. The peak interspike intervals were slightly shorter for ADS (5–7 ms) compared with OLS (7–9 ms), although this was not formally tested. Thus, although more spikes were discriminated in the RFA in the ADS

group, there is no indication of a qualitatively different spiking pattern (e.g., short-interval bursting patterns; Fig. S6*C*).

Poststimulus spike firing rates. LMMs detected higher spike firing rates in the ADS group than the OLS group in the stimulation ON condition ($P < 0.0001$; Fig. 4). Firing rates differed statistically in the OFF condition between groups ($P = 0.0230$) because they increased for the ADS group and decreased slightly for the OLS group, but this qualitative interaction was such that the firing rate trajectories for the groups crossed at approximately 1 wk (Fig. 4*B* and Fig. S6*B*). The ADS group had consistently higher ON vs. OFF spike firing rates than the OLS group over time ($P = 0.0003$).

Lesion Size. Cortical lesions created by the CCI were comparable both qualitatively and quantitatively to those reported in a previous study in this laboratory (2). In all cases, the lesion was confined to the CFA and immediately surrounding tissue. No damage was evident under light microscopy in the RFA in any of the cases. No statistical differences were detected across the three treatment groups [$\chi^2(2) = 1.22$; $P = 0.543$]. The means (SDs) for the ADS, OLS, and control groups were 20.16 (7.75), 20.93 (4.61), and 17.30 (6.84) mm^3, respectively.

SI Discussion

A number of questions remain to be answered following this demonstration of virtually complete recovery of function achieved via closed-loop stimulation. First, can the same results be demonstrated using similar theta-burst parameters in an open-loop mode of stimulation? Although this would simplify therapeutic approaches, it is likely that this approach would result in nonspecific potentiation with regard to target. Virtually every cortical and subcortical structure receiving connections from the stimulation site would be equally potentiated. By triggering stimulation from a specific location, it is likely that spike timing-dependent plasticity mechanisms shape the sign and magnitude of potentiation at each site (9). The complex anatomy of cortical circuits and the reciprocity of corticocortical pathways render a more specific model challenging. However, by using intrinsic neuronal firing patterns in chronic ambulatory models to define stimulation protocols, it may be possible to optimize brain stimulation approaches for therapeutic applications after brain injury.

It is also not clear if ADS induces specific anatomical changes. Because substantial axonal sprouting occurs spontaneously after a focal cortical insult (10) and at least in nonhuman primates, new synaptic connections form between PM and somatosensory cortex after a primary motor cortex injury (11), it is possible that ADS modulates this process. Tract-tracing studies have shown that at least some reciprocal connections exist normally between the RFA and S1 in rats (12). Low-frequency synchronous oscillatory activity appears to be necessary for novel postinjury sprouting to occur (13). Thus, ADS may promote spontaneously sprouting axons to terminate in areas with high temporal correlation. Although anatomical changes cannot be ruled out, the rapid behavioral gains and functional connectivity observed in this study suggest that physiological changes in synaptic efficacy, either between cortical areas or across broader cortical and subcortical networks, underlie the recovery. Thus, potentiation of existing synapses is plausible and perhaps the most parsimonious explanation, given the rapid increase in stimulus-evoked spikes within the first day of microdevice operation. Although at least some of the short-latency spike events observed with ADS (range: 4–6 ms) are consistent with monosynaptic corticocortical connections, it is more likely that changes occur in a broader neuronal network, due to the persistence of increased spiking throughout the 28-ms poststimulus window.

Finally, a third question concerns the longevity of the effect. Although there was some decay in behavioral performance on day 28, whether this was due to nonfunctioning devices (which would suggest a temporary effect of ADS on performance) will require formal study. Based on prior studies, effects may not be long-lasting (14–16). Additional experiments tracking behavioral performance for extended time periods following discontinuation of ADS would be needed. Also, correlation of spike activity recorded simultaneously from S1 and the RFA would be needed to assess functional connectivity further in the absence of stimulation.

1. Kleim JA, Barbay S, Nudo RJ (1998) Functional reorganization of the rat motor cortex following motor skill learning. *J Neurophysiol* 80(6):3321–3325.
2. Nishibe M, Barbay S, Guggenmos D, Nudo RJ (2010) Reorganization of motor cortex after controlled cortical impact in rats and implications for functional recovery. *J Neurotrauma* 27(12):2221–2232.
3. Urban ET, 3rd, et al. (2012) Gene expression changes of interconnected spared cortical neurons 7 days after ischemic infarct of the primary motor cortex in the rat. *Mol Cell Biochem* 369(1-2):267–286.
4. Azin M, Guggenmos DJ, Barbay S, Nudo RJ, Mohseni P (2011) A miniaturized system for spike-triggered intracortical microstimulation in an ambulatory rat. *IEEE Trans Biomed Eng* 58(9):2589–2597.
5. Azin M, Guggenmos DJ, Barbay S, Nudo RJ, Mohseni P (2011) A battery-powered activity-dependent intracortical microstimulation IC for brain-machine-brain interface. *IEEE J Solid-State Circuits* 46(4):731–745.
6. Vicente R, Gollo LL, Mirasso CR, Fischer I, Pipa G (2008) Dynamical relaying can yield zero time lag neuronal synchrony despite long conduction delays. *Proc Natl Acad Sci USA* 105(44):17157–17162.
7. Park HJ, et al. (2013) Semi-automated method for estimating lesion volumes. *J Neurosci Methods* 213(1):76–83.
8. McCulloch CE, Searle SR (2001) *Generalized, Linear, and Mixed Models* (Wiley, New York).
9. Feldman DE (2012) The spike-timing dependence of plasticity. *Neuron* 75(4):556–571.
10. Carmichael ST (2003) Plasticity of cortical projections after stroke. *Neuroscientist* 9(1):64–75.
11. Dancause N, et al. (2005) Extensive cortical rewiring after brain injury. *J Neurosci* 25(44):10167–10179.
12. Urban ET, 3rd, Nishibe M, Barbay S, Guggenmos DJ, Nudo RJ (2013) Afferent and efferent cortical connections of the rostral forelimb area in rat. *2013 Neuroscience Meeting Planner* (Society for Neuroscience, New Orleans), Program No. 173.09. Available at http://www.sfn.org/~/media/SfN/Documents/Annual%20Meeting/FinalProgram/FullAbstractPDFs/AbstractPDFs_Poster_Sun_AM.ashx.
13. Carmichael ST, Chesselet MF (2002) Synchronous neuronal activity is a signal for axonal sprouting after cortical lesions in the adult. *J Neurosci* 22(14):6062–6070.
14. Jackson A, Mavoori J, Fetz EE (2006) Long-term motor cortex plasticity induced by an electronic neural implant. *Nature* 444(7115):56–60.
15. Rebesco JM, Miller LE (2011) Enhanced detection threshold for in vivo cortical stimulation produced by Hebbian conditioning. *J Neural Eng* 8(1):016011.
16. Rebesco JM, Stevenson IH, Körding KP, Solla SA, Miller LE (2010) Rewiring neural interactions by micro-stimulation. *Front Syst Neurosci* 4, 10.3389/fnsys.2010.00039.

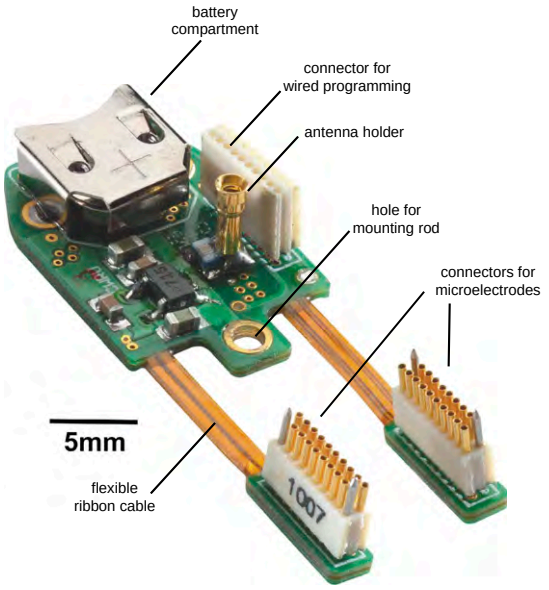

Fig. S1. Photograph of the microdevice used in ADS and OLS experiments. This top view shows the battery compartment, on-board Omnetics connector for wired programming, gold pin as the antenna holder, and hole for mounting to the skull using a stainless-steel threaded rod. Other essential electronic components are shown mounted onto the circuit board. Also, two flexible ribbon cables lead to male Omnetics connectors that mate with female connectors leading to recording and stimulating microelectrodes. A custom-designed integrated circuit and some external components are located on the underside of the circuit board and are not shown. Further microdevice details are provided in prior publications (4, 5).

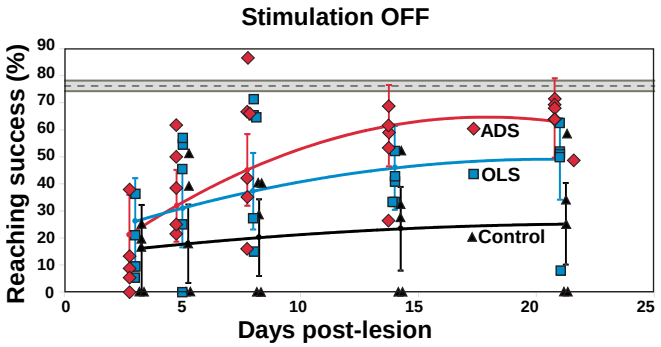

Fig. S2. Performance of rats on a skilled reaching task after injury to primary motor cortex (OFF condition). The ADS group is shown in red, the OLS group is shown in blue, and the control group is shown in black. The dotted line indicates the average prelesion performance of all animals in the study. The bounded area indicates the 95% confidence interval. Regression lines are based on an LMM (8). Error bars represent 95% confidence intervals. Recovery profiles of the ADS and OLS groups in the OFF condition were similar to those of the ON condition (Fig. 3). However, due to the differences in the ON vs. OFF conditions noted for the ADS group during early postlesion days, the OFF condition shows a slightly less rapid recovery. In contrast, rats in the OLS group tended to perform slightly better when the stimulation was OFF. Therefore, their recovery appears a bit more rapid compared with the ON condition. Reaching success differed across treatment groups even in the OFF condition on postlesion day 8 (global comparisons: $P = 0.0229$; pairwise comparisons: $P = 0.3845$ for ADS vs. OLS, $P = 0.0069$ for ADS vs. control, and $P = 0.0686$ for OLS vs. control), day 14 (global comparisons: $P = 0.0014$; pairwise comparisons: $P = 0.1246$ for ADS vs. OLS, $P = 0.0003$ for ADS vs. control, and $P = 0.0316$ for OLS vs. control), and day 21 (global comparisons: $P = 0.0010$; pairwise comparisons: $P = 0.1571$ for ADS vs. OLS, $P = 0.0002$ for ADS vs. control, and $P = 0.0186$ for OLS vs. control). Although the ADS and OLS groups did not differ significantly on any day in the OFF condition, the ADS group performed significantly better than the control group on days 8, 14, and 21, whereas the OLS group performed significantly better than the control group only on days 14 and 21 (pairwise comparisons). This suggests that even in the OFF condition, the ADS group improved faster ($P < 0.05$; ON condition results are provided in the main text). Small symbols represent individual animal data points. One rat in the ADS group was tested on postlesion day 22; thus, the data point is offset.

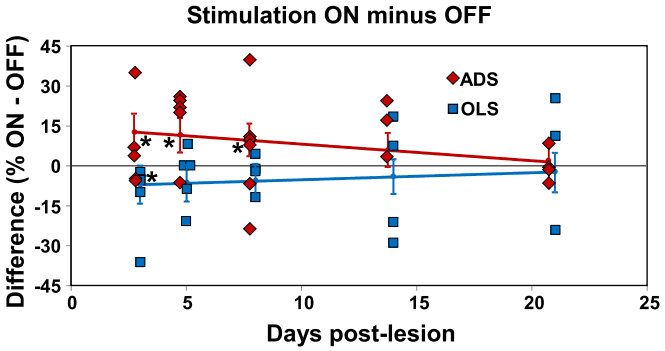

Fig. S3. Comparison of motor performance on the skilled reaching task in OFF vs. ON conditions. The ADS group is shown in red, and the OLS group is shown in blue. Error bars represent 95% confidence intervals. Only rats that were tested in both ON and OFF conditions are included. If the microdevice was not functional, those rats were excluded for that particular day. *$P < 0.05$ (within-group ON/OFF comparisons). Diamonds and squares represent individual animal data points.

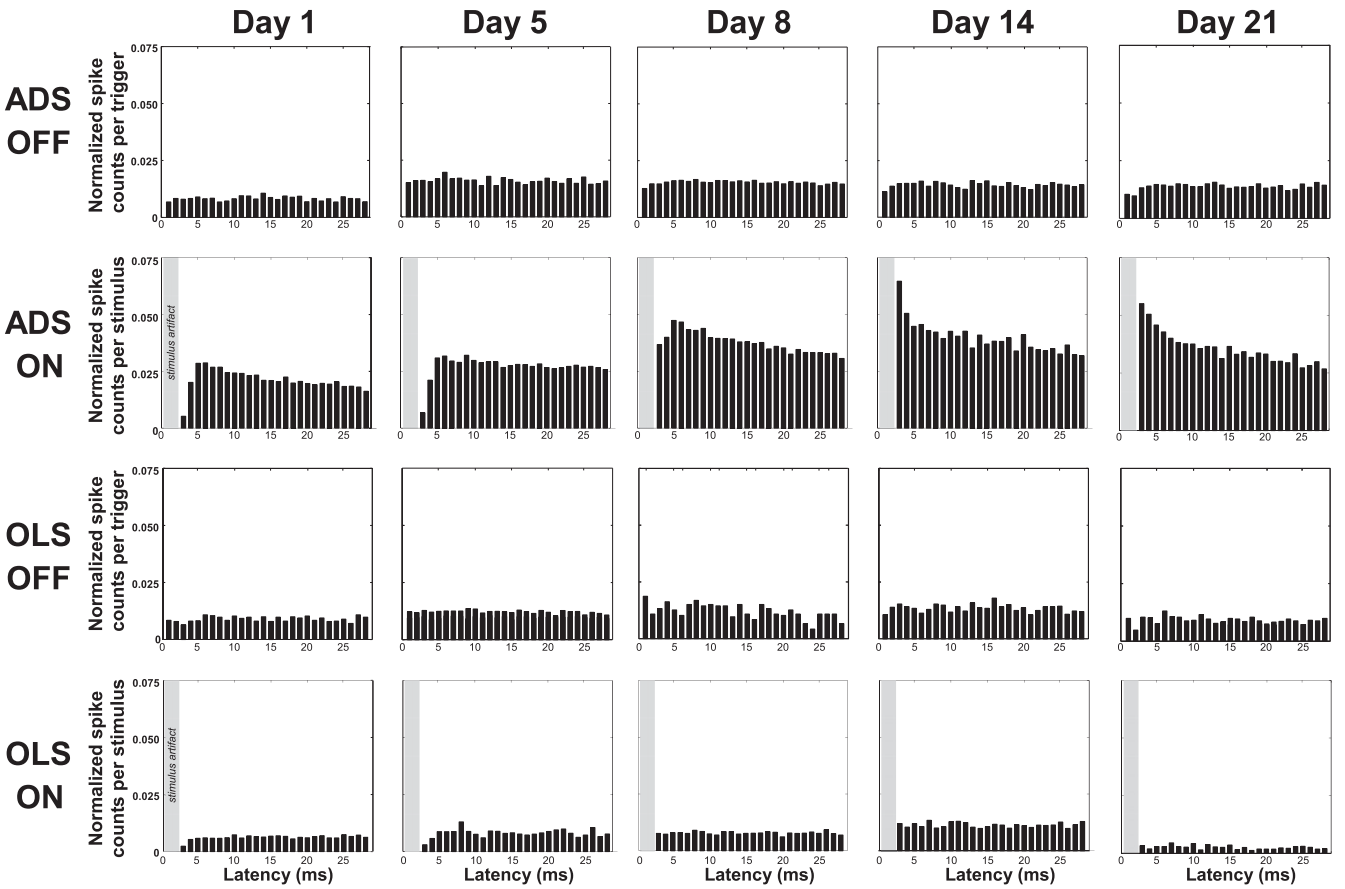

Fig. S4. Poststimulus spiking histograms derived from neural recordings in the RFA on days 1, 5, 8, 14, and 21 (±1 d). This figure is intended to show data on the initial day of microdevice operation (after spike discrimination parameters were initially set), as well as on a schedule closely approximating behavioral testing days. Data were pooled across subjects for each day. Data in ON conditions represent spikes discriminated in the RFA after an intracortical stimulus in S1. Data in OFF conditions represent spikes discriminated in the RFA after an initial trigger spike (in the RFA). Histograms portray the average number of action potentials (spikes) discriminated from the neural recordings within each 1-ms bin. That is, in the ADS ON condition, the data were normalized to the total number of ADS events (by definition, equal to the number of activity-dependent trigger events) in S1. In the OLS ON condition, the data were normalized to the total number of random stimulation events. In the OFF condition, the data were normalized to the total number of stimulus events that would have occurred if the stimulation circuit had been turned on (thus, the total number of trigger events that would have resulted in stimulation if the stimulation circuit had been turned on). For any given stimulus event in S1, multiple spikes might occur within the 28-ms window or no spikes might occur. The dataset used for the analysis was based on an average of over 22,000 stimulation pulses per animal per day. In the ON condition, the data were normalized to spikes per stimulus pulse. In the OFF condition, the data were normalized to spikes per trigger event. Spike counts remained at relatively low levels in the OLS group throughout the experimental period, regardless of whether the microdevice was ON or OFF. Spike counts in the ADS group were similarly low in the OFF condition. In the ON condition, poststimulus spiking was substantially higher in the ADS group, beginning on day 1. A trend toward increasing spike counts in the ON condition can be seen across days, especially in the earlier time bins (<8 ms).

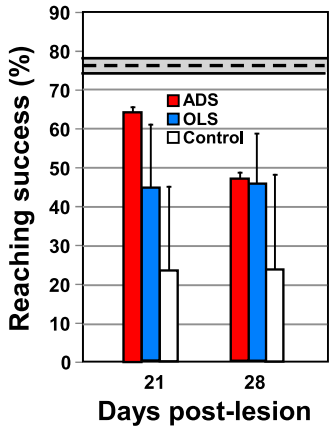

Fig. S5. Comparison of behavioral performance on days 21 and 28 (ON condition). Because only one ADS and three OLS rats had functional microdevices on day 28, these data are displayed separately here (also Table S2). The mean performance in the control group and OLS group remained relatively stable. However, performance in the ADS group dropped from a mean of 64.3% to 47.8%, similar to the performance in the OLS group (mean = 45.8%). Although this phenomenon will require formal study, it suggests that the ADS stimulation is necessary for the enhanced performance to continue. It also suggests that either a longer duration of operation (i.e., beyond 21 d) is required for persistent effects or ADS enhances the rate, but not the extent of recovery, compared with OLS. Error bars represent plus 1 SD. The dotted line indicates the average prelesion performance of all animals in the study. The bounded area indicates the 95% confidence interval.

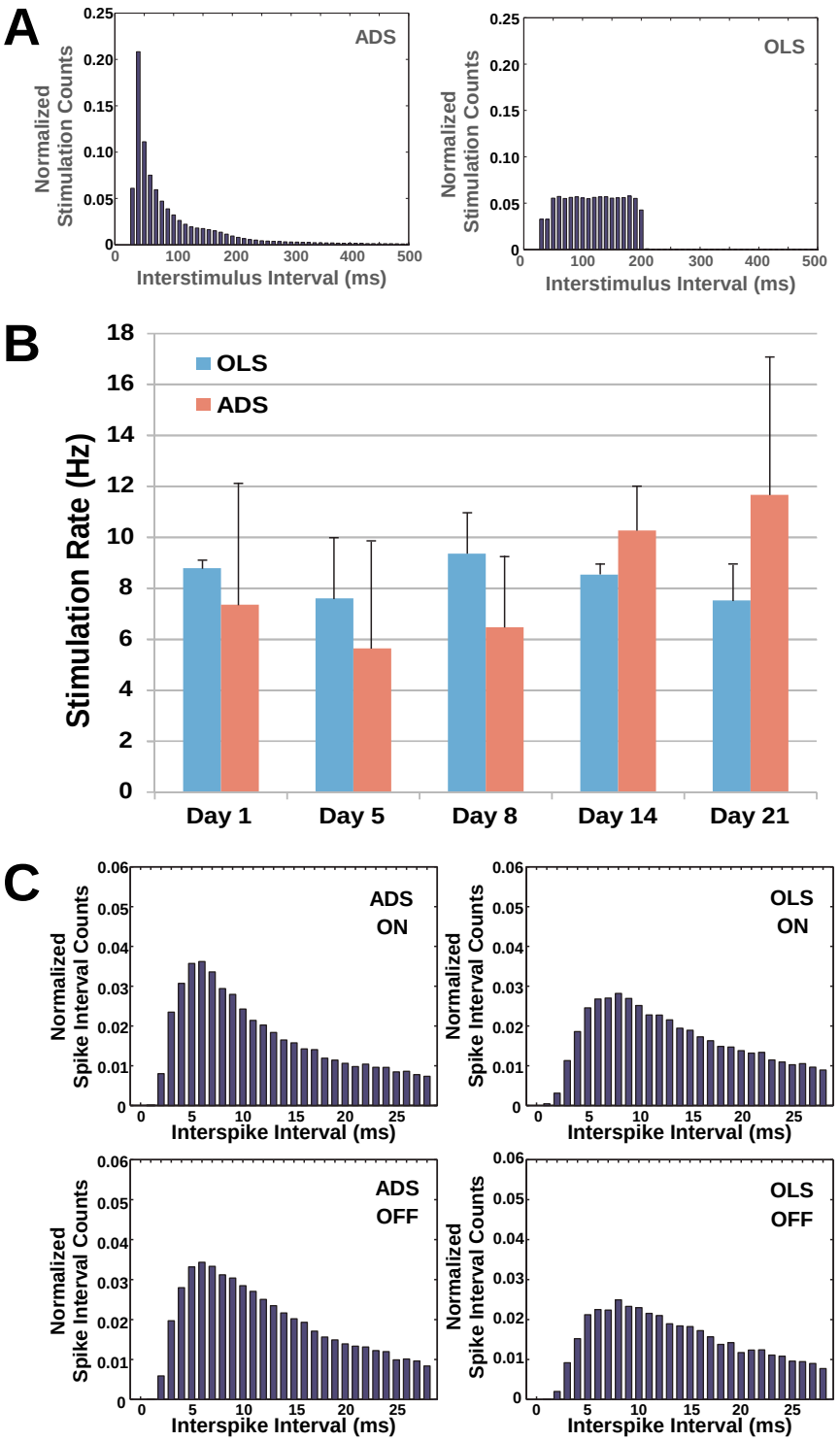

Fig. S6. Stimulation interval distribution, stimulation rate, and poststimulus spike interval distribution in the ADS and OLS groups. (*A*) Interstimulus intervals derived from pooled data on days 1–21. Stimulation counts were normalized to the session length. The interstimulus intervals for the OLS group were defined by the program parameters and intentionally set for equal intervals across the range of intervals most frequently observed in the ADS group. It should be noted that the imposed 28-ms blanking period prevented extremely short interstimulus intervals. Although there were more short interstimulus intervals and fewer long interstimulus intervals in the ADS group, this was a reasonable approximation for equating stimulation parameters within the constraints of the microdevice. (*B*) Average stimulation rates on days 1, 5, 8, 14, and 21 (±1 d). An LMM detected a statistical difference between the groups ($P = 0.0395$); this difference represented a qualitative interaction such that stimulation rates increased for the ADS group and decreased slightly for the OLS group (with their trajectories crossing at approximately 1.5 wk), and the means of these groups overall were quite similar at 8.26 Hz (SD = 3.86 Hz) for ADS and 8.18 Hz (SD = 1.42 Hz) for OLS. Error bars represent plus 1 SD. (*C*) Poststimulus interspike intervals pooled from data on days 1–21. These data were derived from spikes discriminated from recordings in the RFA following an intracortical stimulation pulse in S1. The distribution of interspike intervals is quite similar in the two groups. Although more spikes were discriminated in the RFA in the ADS group, there is no indication of an unusual spiking pattern (e.g., short-interval bursting patterns).

Table S1. Microdevice replacements

Group	Problem	Remedy	Day of discovery/repair
ADS	No recorded signal	Microdevice replacement	4
ADS	Intermittent signal/no stimulation	Microdevice replacement	11
ADS	No recorded signal	Microdevice replacement	15

Table S2. Number of rats with functional microdevices on each postlesion testing day

Day	ADS	OLS
3	6	5
5	6	5
8	6	5
14	5*	4†
21	4‡	4
28	1†,‡	3†

Because an intent-to-treat statistical model was used, when a microdevice was no longer functional, the rat was still tested and the data were included in the analysis.

*One rat died between days 8 and 14.

†Repairable microdevice failure, microdevice not replaced (ADS group: day 28, $n = 2$; OLS group: day 14, $n = 1$; day 28, $n = 1$). The microdevice was not replaced if behavioral performance had recovered approximately to normal range. This was necessary largely due to scarcity of microdevices.

‡Nonrepairable microdevice failure (ADS group: day 21, n =1; day 28, $n = 1$).

Movie S1. Videotape clips show representative rats performing the skilled reaching task before and after (postlesion day 8) the traumatic brain injury. Videotape clips are divided into (*i*) prelesion, (*ii*) control (postlesion day 8), and (*iii*) ADS (ON condition, postlesion day 8). In each of the clips, reach sequences were edited to portray the average retrieval performance for the group. In the control rat, severe impairments can be seen as the rat makes substantial trajectory and grasping errors. The rat in the ADS group is seen retrieving pellets similar to the prelesion rat [Quicktime, Apple; 8.2 megabytes (MB)].

Movie S1

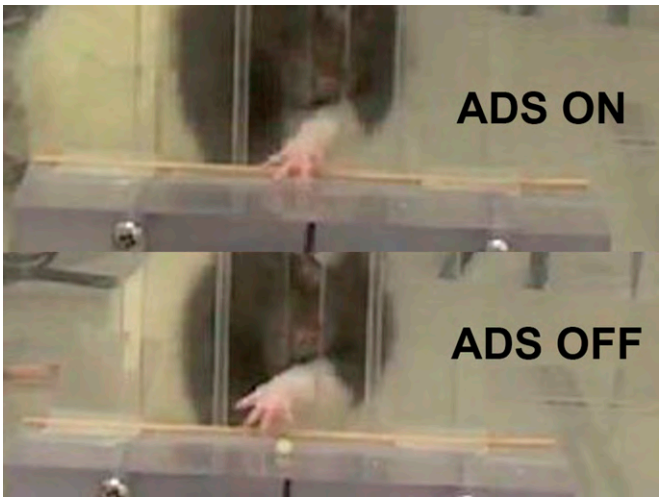

Movie S2. Videotape clips of an individual rat from the ADS group performing the skilled reaching task in the OFF condition and then in the ON condition. In this videotape, the rat is tethered, because all programming functions, including programming the ON or OFF state, must be done through the wired connection. On postlesion day 8, this rat still makes substantial errors in the OFF condition. After the microdevice is turned ON (about 3 min later), the rat immediately begins making successful retrievals. This difference in the OFF vs. ON condition was particularly noticeable in this rat, but the effect was significant in the entire group on postlesion days 3, 5, and 8 (Fig. S4) (Quicktime; 9.2 MB).

Movie S2

Print this Page

Presentation Abstract

Program#/Poster#:	79.06/VV4
Presentation Title:	Potentiating functional connectivity between distant cortical locations with activity dependent stimulation in the anesthetized rat
Location:	Halls B-H
Presentation time:	Saturday, Nov 09, 2013, 2:00 PM - 3:00 PM
Topic:	++D.18.b. Neurophysiology: Implanted electrodes, other direct interactions with neurons
Authors:	***G. M. VAN ACKER, III**[1], D. GUGGENMOS[1], A. PACK[1], C. DUNHAM[2], R. J. NUDO[1,2]; [1]Mol. and Integrative Physiol., [2]Landon Ctr. on Aging, Univ. of Kansas Med. Ctr., Kansas City, KS
Abstract:	Facilitating functional recovery following traumatic brain injury, ischemic stroke and other cortical lesions remains an ongoing clinical challenge. Electrophysiological techniques being investigated to enhance functional recovery, such as transcranial magnetic stimulation, transcranial direct-current stimulation and epidural cortical stimulation have met with limited success (Edwardson et al. 2013). More recently, studies aimed at stimulating reorganization of cortico-muscle connectivity (Lucas et al. 2013) and enhancing functional recovery following cortical lesion by utilizing activity-dependent stimulation (ADS) have shown encouraging results (Guggenmos et al. 2012). The present study expands upon these findings by potentiating functional connectivity between the rostral forelimb area (RFA) and somatosensory cortex (S1) using ADS in the anesthetized rat within a single four-hour recording session. RFA and S1 forelimb area were identified in healthy and ketamine-sedated Long-Evans rats (ages ~7 months). RFA cell activity was recorded using a sixteen-contact electrode distributed on four shanks (A16 4x4, NeuroNexus), and stimulation was applied to a single S1 cortical site using either an ADS (closed loop) or random stimulation (open loop) condition for each rat. For ADS, action potentials recorded at a single contact site from a moderately-firing cell triggered single 200µs, 60µA cathodal-leading biphasic pulses to S1 subsequent to a 10 ms delay. For random stimulation, rather than RFA activity-triggered events, randomized stimuli approximating the frequency observed in the ADS conditions were applied. To prohibit stimulus-activated RFA

spikes and stimulus artifact from triggering stimulation, a short blanking period (29 ms) followed each stimulus. This provided a fixed window within which to observe the resultant evoked activity. Preliminary results reveal that ADS can affect the firing pattern of the RFA-triggering cell relative to triggered S1 stimulation within a single anesthetized recording period. Additionally, ADS-driven facilitation was found to also occur in cells recorded from electrode contacts adjacent to the trigger-cell recording site, suggesting that stimulation may affect the network of cells that are spatially, and likely synaptically, coupled with the trigger-cell. Facilitating connectivity within a short epoch and during anesthetization provides a foundation for rapidly assessing the optimal stimulus parameters for implementing ADS, and may in the future aid directly in facilitation of functional recovery after brain injury.

Disclosures: **G.M. Van Acker:** None. **D. Guggenmos:** None. **A. Pack:** None. **C. Dunham:** None. **R.J. Nudo:** None.

Keyword(s): MOTOR CORTEX

PLASTICITY

STIMULATION

Support: DoD W81XWH-10-1-0742

Landon Center on Aging Endowments

Print this Page

Presentation Abstract

Program#/Poster#:	79.12/VV10
Presentation Title:	Neuroelectrophysiological effects of activity-dependent stimulation following a controlled cortical impact to primary motor cortex of the rat
Location:	Halls B-H
Presentation time:	Saturday, Nov 09, 2013, 4:00 PM - 5:00 PM
Topic:	++D.18.b. Neurophysiology: Implanted electrodes, other direct interactions with neurons
Authors:	***D. J. GUGGENMOS**[1], C. DUNHAM[2], M. AZIN[4], S. BARBAY[2], J. D. MAHNKEN[3], P. MOHSENI[4], R. J. NUDO[2]; [1]Dept. of Mol. and Integrative Physiol., [2]Landon Ctr. on Aging, [3]Dept. of Biostatistics, Univ. of Kansas Med. Ctr., Kansas City, KS; [4]Dept. of Electrical Engin. and Computer Sci., Case Western Reserve Universtiy, Cleveland, OH
Abstract:	Following a unilateral injury to primary motor cortex (M1), reorganization in spared motor cortical areas is thought to restore some of the lost functionality resulting from the lesion. Further, disruption of sensorimotor integration influences the severity of motor deficit. Previously, we have shown that recovery of function following M1 injury in a rat model of traumatic brain injury is enhanced by establishing an artificial sensorimotor communication link between the spared rostral forelimb area (RFA, a premotor area) and the forepaw area of the primary somatosensory cortex (S1). This approach used activity-dependent stimulation (ADS) to artificially link the two areas. Detection of action potentials (spikes) in RFA triggered electrical stimulation in S1 to promote Hebbian plasticity. In the present study, we sought neurophysiological evidence that communication between RFA and S1 was altered by ADS. Rats were given a traumatic brain injury by controlled cortical impact (CCI) over the forelimb area of M1. The animals were then implanted with recording electrodes in RFA and stimulating electrodes in S1. A wireless, battery-operated, custom-built microdevice was then attached to the electrodes and set to deliver either activity-dependent stimulation (ADS, N=6) or randomized, open-loop stimulation (OLS, N=5) up to 24 hours daily for 28 days following the CCI. Stimulation parameters were such that detected spikes in PM would trigger a single 200µs pseudo-biphasic 60µA stimulation pulse in S1 after a

7.5ms delay. A 28ms blanking period from initial detection of the spike provided a fixed time window to observe evoked neural activity in RFA following the S1 stimulation pulse. Both groups received similar amounts of stimulation (ADS = 8.26Hz ± 3.86Hz; OLS = 8.18Hz ± 1.42Hz) and had similar inter-spike intervals. ADS, but not OLS, led to a change in the firing rate of the neurons recorded in RFA used to trigger the stimulation. That is, in the ADS group, but not the OLS group, there was a significant increase in spikes in RFA in the 28ms following the S1 stimulation pulse compared to periods when the stimulation was off ($p < 0.0001$). The increase in stimulus-evoked spikes was observed within hours upon the initiation of ADS, and persisted for the duration of the experiment (up to 28 days). Taken together with the previous behavioral results, these data demonstrate that following a lesion to M1, communication between two distant areas (RFA and S1) can be facilitated using ADS, and that this artificial communication link aids in recovery. This demonstration may have substantial implications in development of closed-loop therapeutic interventions following cortical injury.

Disclosures: **D.J. Guggenmos:** None. **S. Barbay:** None. **C. Dunham:** None. **J.D. Mahnken:** None. **P. Mohseni:** None. **M. Azin:** None. **R.J. Nudo:** None.

Keyword(s): ELECTROPHYSIOLOGY

RAT

TRAUMATIC BRAIN INJURY

Support: DoD CDMRP W81XWH-10-1-0741 (PM)

NIH W81XWH-10-1-0742 (RJN)

Landon Center on Aging Endowments

Print this Page

Presentation Abstract

Program#/Poster#:	17.08
Presentation Title:	Inducing cortico-cortical connectivity to bypass acute cortical impact injury in the rat
Location:	WCC 143A
Presentation time:	Saturday, Nov 15, 2014, 2:45 PM - 3:00 PM
Topic:	++D.10.d. Plasticity: Neurophysiology
Authors:	***G. M. VAN ACKER, III**[1], D. GUGGENMOS[1], S. BARBAY[1], K. CRABTREE[2], C. DUNHAM[1], R. J. NUDO[1]; [1]Mol. and Integrative Physiol., [2]Neurosurg., Univ. of Kansas Med. Ctr., Kansas City, KS
Abstract:	Reconstruction of neural circuitry following acute central nervous system injury remains an ongoing clinical and basic research challenge. Recent studies that applied activity-dependent stimulation (ADS) to promote functional recovery following cortical lesion (Guggenmos et al. 2013) and to entrain cortico-cortical connectivity in the intact brain (Van Acker III et al. 2013) provide encouraging results. The present study expands upon these results by utilizing ADS to potentiate cortico-cortical connectivity immediately status-post controlled cortical impact (CCI) lesion to the caudal forelimb area (CFA) within primary motor cortex. Subsequent to impact in each of 16 ketamine-sedated Long-Evans rats, stimulation was delivered to either somatosensory (S1) forelimb or barrel field (BF) areas using either ADS (n= 8 rats) or random stimulation (RS; n= 8 rats) for 180 minutes. For ADS, neural activity recorded from rostral forelimb area (RFA) was used to trigger stimulus pulses, whereas RS pulses were delivered independent of biological feedback at approximately 7 Hz (Gaussian distribution). Results suggest that cortico-cortical entrainment immediately status-post CCI injury can be evoked more readily than in the healthy brain (Van Acker III et al. 2013), dependent upon location of cortical stimulation. For example, when ADS was delivered to BF in the injured brain, spikes that occurred within 28 ms following each stimulus pulse

(spikes/stimulus) increased significantly from the first 30 minutes of stimulation (5.3 ± 1.5 spikes/stimulus) to the final 30 minutes (12.3 ± 1.4 spikes/stimulus, $p < 0.05$), an increase of 7.0 ± 2.7 spikes/stimulus. In contrast, when stimulation was delivered to BF in the healthy brain, the difference in stimulus-associated spikes between the first and last 30 minutes was not significant (0.7 ± 0.7 spikes/stimulus, $p < 0.05$) (Van Acker III et al. 2013). Additionally, when stimulation was delivered to S1 in the injured brain, there was no significant increase in activity between the first and last 30 minutes (3.0 ± 1.1 and 3.5 ± 2.3 spikes/stimulus, respectively; $p > 0.05$). The difference in potentiation of connectivity between S1 and RFA compared to BF and RFA may be due to differences in preexisting connectivity between the two pathways. There are known direct connections between S1 and RFA, whereas there are minimal-to-no direct connections between BF and RFA. It is possible that immediately status-post CCI, a diaschisis-like effect may have differentially disrupted the neurophysiological integrity of S1-RFA cortico-cortical neurons, resulting in an inability to potentiate functional connectivity.

Disclosures: **G.M. Van Acker:** None. **D. Guggenmos:** None. **S. Barbay:** None. **K. Crabtree:** None. **C. Dunham:** None. **R.J. Nudo:** None.

Keyword (s): SENSORIMOTOR

MOTOR CORTEX

PLASTICITY

Support: DoD Award W81XWH-10-1-0741

NIH: R37 NS30853